

Review

Recent progress and new challenges in modeling of human pluripotent stem cell-derived blood-brain barrier

Li Yan¹✉, Rebecca A. Moriarty¹, Kimberly M. Stroka^{1,2,3,4}✉

1. Fischell Department of Bioengineering, University of Maryland, College Park, MD 20742, USA
2. Biophysics Program, University of Maryland, College Park, MD 20742, USA
3. Center for Stem Cell Biology and Regenerative Medicine, University of Maryland, Baltimore, MD 21201, USA
4. Marlene and Stewart Greenebaum Comprehensive Cancer Center, University of Maryland, Baltimore, MD 21201, USA

✉ Corresponding authors: Dr. Li Yan; liyan12@umd.edu. Dr. Kimberly M. Stroka.

© The author(s). This is an open access article distributed under the terms of the Creative Commons Attribution License (<https://creativecommons.org/licenses/by/4.0/>). See <http://ivyspring.com/terms> for full terms and conditions.

Received: 2021.05.26; Accepted: 2021.10.05; Published: 2021.11.02

Abstract

The blood-brain barrier (BBB) is a semipermeable unit that serves to vascularize the central nervous system (CNS) while tightly regulating the movement of molecules, ions, and cells between the blood and the brain. The BBB precisely controls brain homeostasis and protects the neural tissue from toxins and pathogens. The BBB is coordinated by a tight monolayer of brain microvascular endothelial cells, which is subsequently supported by mural cells, astrocytes, and surrounding neuronal cells that regulate the barrier function with a series of specialized properties. Dysfunction of barrier properties is an important pathological feature in the progression of various neurological diseases. *In vitro* BBB models recapitulating the physiological and diseased states are important tools to understand the pathological mechanism and to serve as a platform to screen potential drugs. Recent advances in this field have stemmed from the use of pluripotent stem cells (PSCs). Various cell types of the BBB such as brain microvascular endothelial cells (BMECs), pericytes, and astrocytes have been derived from PSCs and synergistically incorporated to model the complex BBB structure *in vitro*. In this review, we summarize the most recent protocols and techniques for the differentiation of major cell types of the BBB. We also discuss the progress of BBB modeling by using PSC-derived cells and perspectives on how to reproduce more natural BBBs *in vitro*.

Key words: blood-brain barrier, pluripotent stem cells, brain microvascular endothelial cells, neurovascular unit, disease modeling.

Introduction

The blood-brain barrier (BBB) is a highly selective barrier that is comprised of endothelial cells and that separates the brain parenchyma from peripheral blood. This barrier restricts the access of hydrophilic molecules and leukocytes from the blood into the central nervous system (CNS), thereby playing a critical role in protecting neuronal tissue and maintaining brain homeostasis [1]. The breakdown of the BBB leads to the entry of toxins and pathogens, as well as infiltration of immune cells into the CNS, subsequently contributing to neurological imbalance. BBB dysfunction is involved in the pathogenesis of many neurological diseases, including stroke, trauma, multiple sclerosis, Parkinson's disease (PD), and Alzheimer's disease

(AD) [2]. This is further compounded by the fact that the BBB is a major obstacle for the CNS drug delivery. Certain small lipid-soluble drugs with molecular weight under 400 Da may cross the BBB via transmembrane diffusion [3], but over 90% of CNS drugs are not transported across the BBB to enter the CNS, thus impeding the treatment of neurological diseases [4, 5].

The neurovascular unit (NVU) is considered to be a broader structural basis than the BBB and is used to describe the interplay between the blood and the brain. The NVU consists of brain microvascular endothelial cells (BMECs) connected by cell-cell junctions, which line the blood vessels and interact closely with an encapsulating layer of mural cells

(pericytes and vascular smooth muscle cells (SMCs)), astrocytes, as well as other surrounding neural cells. Combined with the basement membrane, these cells form a dynamic system that maintains the cerebrovascular integrity and transduce biochemical and biomechanical signals to regulate the BBB's functions [6]. The physical barrier system restricts the nonspecific transport of large and small molecules across the BBB. It is also the major limiting factor for the therapeutic drugs that aim to penetrate the brain. Despite these limitations, specialized endogenous transport mechanisms exist to enable the transcytosis of molecules entering the CNS to maintain the brain homeostasis. Vesicular-based transport systems such as receptor mediated transcytosis (RMT) have become long-standing strategies for the delivery of therapeutics and biologics to the CNS [3, 7].

Primary cell lines from brain tissues such as primary BMECs, pericytes, and astrocytes are widely used to construct the NVU and investigate the BBB function *in vitro*. However, these primary cells are usually isolated during a brain biopsy, leading to a high degree of batch-to-batch difference. Obtaining a large cell number and retaining BBB properties during proliferation *in vitro* are challenging. In culture, primary NVU cells lose some of their key phenotypes over several passages, and the expression of specific transporters, enzymes, and trans-endothelial electrical resistance (TEER) values are much lower than that of *in vivo* cells. As a result, the scalability of primary cells is limited. It is also not ethical or practical to isolate large amounts of primary cells from human patients, which limits the personalized or industrial BBB development *in vitro* [8].

Recent advances in the field of human pluripotent stem cells (hPSCs) make it possible to provide a robust and scalable cell source for BBB modeling [9-13]. hPSCs derived from healthy and diseased patients can be an ideal alternative to primary cell or animal models for human diseases *in vitro* [14]. hPSCs, including human embryonic stem cells (hESCs) and induced pluripotent stem cells (iPSCs), can differentiate into various NVU cell types such as BMECs, pericytes and astrocytes, which can be assembled into an *in vitro* BBB model. In addition to NVU cells, other cell types such as mesenchymal stem cells (MSCs) can also improve the stabilization of BBB [15, 16]. Previous studies creating hPSC-BBB constructs proved to recapitulate the complex BBB function *in vitro*, such as well-formed tight junction protein expression which led to physiologically equivalent TEER values [17]. Recent hPSC-BBB models also display various adhesion molecules that are suitable for the study of immune cell migration across the BBB [9]. Due to the expression of proper

transporter proteins, BBB models have been used for predicting permeability of CNS drugs [18]. Thus, BBB models derived from hPSCs provide an important platform for high-throughput screening of brain-penetrating molecules [18]. Furthermore, the isogenic personalized BBB models derived from patient-specific iPSCs can improve our understanding of the BBB in both physiological and pathological conditions [19].

In this review, we provide an overview of PSC-derived BBB models. We first detail the specialization of the BBB and discuss its unique characteristics. Then, we summarize the recent differentiation protocols for major cell types that contribute to barrier function. Next, we illustrate how these cell types are harnessed to engineer PSC-derived BBB models, including transwell, organoids and microfluidic BBB-on-chip systems. Finally, we discuss the personalized BBB modeling of CNS diseases and provide perspectives on how to improve the hPSC-derived BBB modeling *in vitro* and discuss critical questions in the field that require further investigation.

1. Structure and physiology of BBB

The barrier layers of the CNS separate the blood and neural tissues, which synergistically contribute to maintaining brain homeostasis. There are three barriers in the brain, including the BBB, the blood-cerebrospinal fluid barrier, and the epithelial cells of the arachnoid membrane at the brain surface. The BBB is a vast network of over 650 kilometers of small capillaries, of which the average diameter is about 5-8 μm [20, 21]. The NVU at the capillary level is composed of BMECs, astrocyte end-feet, and pericytes embedded in the capillary basement membrane, which also interact with surrounding neuronal cells (Figure 1). This dynamic system allows the flux of various molecules which is crucial to maintain normal brain function [6].

1.1 BMECs

BMECs are specialized endothelial cells lining the microvasculature of the CNS. BMECs are the main player in forming the physical, transport and metabolic barrier restricting the movement of molecules and immune cells between the blood and brain. A continuous sealed BMEC capillary gives rise to a complex and dynamic barrier which limits paracellular transport and diffusion of molecules, ions, and proteins and maintains apical-basal polarity [22]. The properties of this barrier are determined by junctional complexes between adjacent BMECs comprised of tight junctions, adherens junctions, and gap junctions. Tight junctions consist of integral

membrane proteins and several accessory proteins, such as Occludin, Claudins, junction adhesion molecules, and zonula occludens (ZO) proteins. These transmembrane adhesion proteins are arranged parallel to the direction of blood flow and link to the actin cytoskeleton to provide structural support that maintains the BBB integrity [23]. Adherens junctions are composed of two families of transmembrane proteins: cadherins and nectins [24, 25]. By cooperating with afadin and catenin, they form two structurally adhesive units: the cadherin-catenin complex and the nectin-afadin complex. Both mediate cell-cell adhesions and provide scaffolding for tight junction formation. The interactions between ZO-1 and catenin or afadin influence tight junction assembly and reinforce the barrier function [26]. Gap junction intercellular communication is formed by two hemichannels which are composed of six transmembrane connexins proteins. Unlike tight and adherens junction proteins, connexins do not form a tight seal between the adjacent cells. Connexins mediate intercellular communication, which is regulated by pH, voltage, calmodulin and phosphorylation [27], and the opening of connexin hemichannels is controlled in a Ca^{2+} -dependent manner [28]. Due to these well-formed junctional complexes, BMEC monolayers have high TEER values; this differs from other peripheral endothelial cells. The physiological TEER value of brain capillary is $>1000 \Omega \text{ cm}^2$ which is much higher than $3\text{--}33 \Omega \text{ cm}^2$ in other tissues [29].

1.2 Pericytes

Pericytes are branched cells present along the basal wall of capillary blood vessels throughout the body. Although pericytes are widely distributed throughout all organs of the entire body, the density of pericytes varies in different organs and vascular beds, and CNS vasculature is generally regarded as the most pericyte-covered district with an approximately 1:1 to 1:3 pericytes-to-endothelial cells ratio [30]. In the CNS, pericytes play important roles in angiogenesis, neovascularization, maintenance of the BBB integrity and homeostasis, regulation of immune cell infiltration, and control of cerebral blood flow. Pericyte deficiency by mutants of platelet-derived growth factor- β (PDGF β) impairs BBB function by increasing brain vessel permeability, causing abnormal polarization of astrocyte end-feet, and reducing astrocyte-derived basement membrane component Lama2 [31]. The communication between brain endothelial cells and pericytes plays an important role in maintaining the integrity of BBB. This communication is mediated by paracrine signals such as transforming growth factor beta, PDGF-BB, angiopoietin 2, and vascular endothelial growth factor. These factors also affect the survival and contractility of pericytes [32]. In addition, the interaction of pericytes and astrocytes stabilize BBB function. Astrocytic laminin regulates pericyte differentiation from a contractile stage to a resting stage, and thus contributes to BBB integrity [33]. Furthermore, apolipoprotein secreted by astrocytes binds to the receptor on pericytes altering BBB permeability [34].

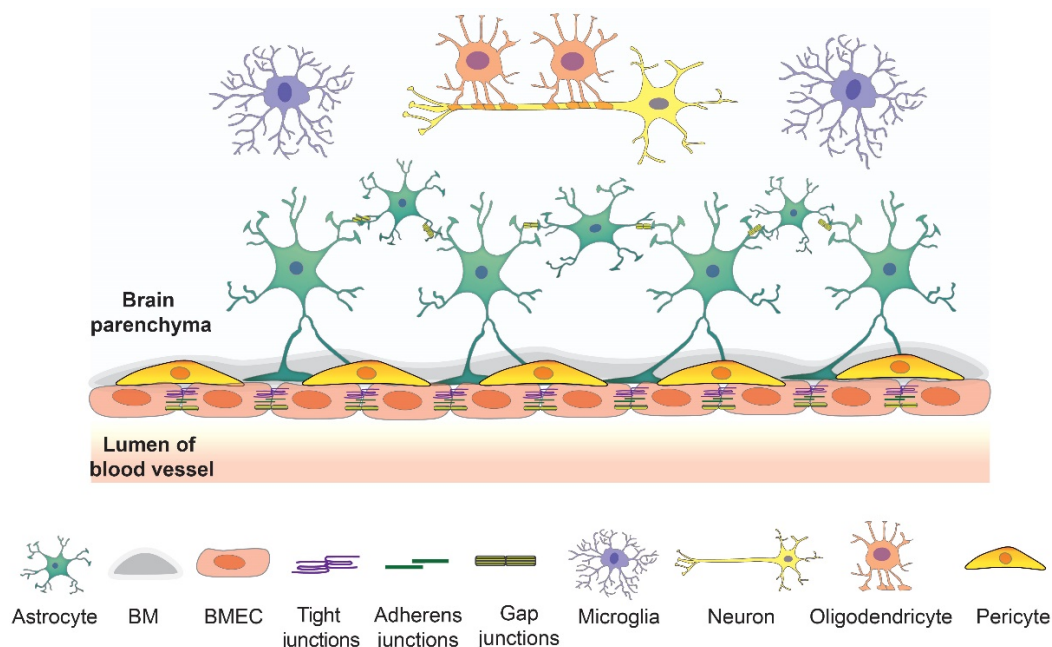


Figure 1. The overview of the components of NVU. BMECs connected by junction proteins intimate contact astrocytes and astrocytes in basement membrane creating a strong barrier. This barrier interacts with other brain cell types such as neurons, microglia, and oligodendrocytes to maintain the brain homeostasis.

1.3 Astrocytes

Astrocyte cells are a heterogeneous population with distinct morphology and function, depending on their specific brain regions in the CNS. They are the most abundant glial cell type in the CNS and play critical roles in the formation and modulation of functional synapses, elimination of toxins and debris, and maintenance of BBB coupling with endothelial cells and pericytes [35]. Astrocytes encircle the vasculature of the CNS with their end feet, which anchor the subendothelial basal lamina and secrete a complex array of biomolecules in the basal lamina influencing endothelial cells and other surrounding cells. A highly specialized astrocyte-endothelial interface is established through inductive processes and direct interaction. Endothelial cells promote the water channel, aquaporin-4 (AQP-4), accumulation in astrocytes' endfeet by compounds they secrete in the extracellular matrix (ECM), such as agrin, as well as direct mechanical interaction with the end feet [36]. Gap junction-mediated intercellular communication is also a typical feature of astrocytes. The connexin gap junction channels on astrocyte end feet mediate the cross-talk between different counterparts of the BBB via Ca^{2+} signaling [27]. Astrocytes also have the ability to respond to and regulate brain inflammation. Astrocytes acquire different phenotypes when they react to different pathological stimuli. The proinflammatory astrocytes secrete pro-inflammatory factors that increase BBB permeability and leukocyte infiltration, which are particularly related to the brain pathologies of diverse neurodegenerative diseases [37, 38]. In contrast, the newly formed reactive astrocytes in glial scars repair the BBB and restrict the inflammatory cells entering the injury or stroke site within the CNS [39]. In addition, region-specific astrocytes, especially in white matter and grey matter, show extensive functional differences, such as different expression of transporters and responses to stimuli, which affect the BBB phenotypes and contribute to BBB heterogeneity [40].

1.4 Basement membrane

The basement membrane surrounding the vascular tube is a unique ECM supporting the BMECs, pericytes, and astrocytes. The basement membrane exerts important functions by maintaining structural specificity and membrane stability. It provides an anchor for many signaling processes at the vasculature interface, but also provides an additional diffusion barrier for molecules and cells to cross before accessing the neural tissue. The basement membrane is a 30 to 40 nm lamina comprised of secreted molecules including fibronectin, nidogen,

type IV collagens, laminin, heparin sulfate proteoglycans, and other glycoproteins. The composition of these ECM proteins changes in the microenvironment of the BBB at different development stages or disease [41]. Meanwhile, disruption of the basement membrane increases BBB permeability and leads to leukocyte infiltration and BBB dysfunction [42].

1.5 Transport system of BBB

Due to the presence of a specialized junction network, BMECs effectively restrict free paracellular transport. They express designated transporters and allow extremely low rates of transcellular transport, exerting a higher degree of control to molecular, metabolite, and nutrient exchange across the BBB [43]. The BBB barrier is highly permeable to gaseous molecules such as O_2 , CO_2 , N_2 , H_2O , as well as volatile anesthetics. Small lipophilic molecules can pass the barrier by diffusing across the lipid bilayer membranes along their concentration gradient [44]. Movement of all other molecules across the BBB is dependent on the presence of transporters. Glucose, as the primary energy substrate, enters the brain by carrier-mediated transport, glucose transport protein type 1 (GLUT-1) [45]. Large molecules, such as peptides and proteins, enter the brain by adsorptive mediated transcytosis (AMT) or RMT [46]. Smaller peptides cross the BBB by either nonspecific endocytosis or RMT. BBB receptors such as transferrin receptor (TfR), insulin receptor, lipid transporters (e.g. low-density lipoprotein receptor), solute carrier family transporter, and leptin receptor recognize the circulating protein ligands and transport the bounding ligands into brain parenchyma via RMT [46, 47]. Drug efflux transporters such as P-glycoproteins (Pgp), multidrug-resistance related protein (MRP), and breast cancer resistance protein (BCRP) can actively transport a huge variety of lipophilic drugs out of the cells forming the BBB which limits the access of drug to CNS tissues [48].

2. Development of the BBB

The barrier properties of brain tissue were first demonstrated by the studies of Ehrlich, Franke, Bouffard, and Goldman around the early 1900's. They showed trypan red, methylene blue, and trypan blue can stain all tissues except the nervous system, which indicates that the barrier system existing in the brain and the CNS is unique from the rest of the body [49, 50]. Stern and Gautier reported detailed studies of penetration of a wide range of molecules from blood into brain and proposed the concept of a BBB in 1921 [49]. Thereafter, many dyes and low molecular weight compounds were used to study BBB permeability by

various routes in different species from embryonic stages through adulthood [50]. Grazer and Clemente injected trypan blue into rat embryos from embryonic day 10.5 (E10.5) to birth and found no staining of brain tissue [51]. Similar results were reported by intravascular injection of fluorescently labeled bovine albumin in rat embryos at E15 [52]. This collective evidence demonstrates that BBB formation begins during early embryonic stage. The permeability experiments using small molecules (e.g., sodium ferrocyanide) suggested that the BBB in young animals is leakier and more permeable than in adult animals. Some interpretations of previous data argue that the BBB in embryos, fetus, and neonate is less mature compared with adult [50]. However, interestingly, there has been recent controversy over the degree of maturity and permeability of the developing BBB [49]. The BBB during development displays stage-specific properties [53], and different transporters of the BBB are developmentally regulated [54]. For example, protein levels of ABCB1 were higher at E13 than in the adults [53]. Solute-linked carrier transporters were expressed at higher levels in the fetal choroid plexus compared to that of adults [50]. Mannose 6-phosphate/insulin-like growth factor 2 receptor had high fetal and prenatal levels, followed by decreased postnatal levels [55]. These reports show that higher expression of some transporters is necessary to facilitate rapid nutrient diffusion or prevent the toxin from brain, which may indicate leaky properties of the BBB during early stages is actually more indicative of the functional specialization [49].

In mammals, the specific properties of the BBB are induced during CNS angiogenesis. The development of the brain vascularization begins with angiogenic sprouting from a perineural vascular plexus. The capillaries sprout and invade the neuroepithelium and form a functional vascular network [56]. Meanwhile, the vascular progenitor cells grow into the embryonic neuroectoderm [26]. In the rat cerebral cortex, neuronal angiogenesis begins at E12, approximately halfway through the normal 24-day gestation time. Neural progenitor cells secrete molecular signals such as vascular endothelial growth factor (VEGF) and Wnt that guide the migration of endothelial progenitor cells into the neural tissue from the surrounding vascular plexus towards the ventricles [57, 58]. In mice, the early BBB properties begin at stage E11, including elevated expression of tight junction proteins and efflux transporters, and downregulation of transcytosis (plasmalemma vesicle-associated protein) and leukocyte adhesion molecules (ICAMs) [54]. The expression of GLUT-1 gradually decreases in neuroepithelial cells and

increases in the brain endothelial cells from E12 to E16 in rat brains to meet the increasing demands for glucose [59]. ATP-binding cassette (ABC) efflux pumps such as ABCC and BCRP are expressed at E12.5 in mouse and show apparent change in expression throughout development [60], while Pgp is expressed at low levels during embryogenesis and increases during postnatal development [54]. This indicates that different transporters have different regulation mechanisms during development [60]. The fenestrated parenchymal vessels at E13 and low TEER indicate an incomplete barrier function with high permeability [61]. The maturation of the BBB starts from E13 in intraparenchymal vessels and E17 in pial vessels. At these time points, the fenestration declines rapidly. The TEER value was found to be increased significantly in pial vessels of the rat at E21 [62]. Further analysis in mice indicates tight junction molecules occludin, claudin-5 and ZO-1 are expressed at E12 [54]. The junctional strands are visible in brain capillaries beginning at E13.5 and the BBB becomes tightly restricted between E14.5 and E15.5 [63, 64]. In human brain, tight junction proteins occludin and claudin-5 were first detected at the interface of adjacent endothelium at 14 weeks gestation [65].

During the invasion process, endothelial cells secrete factors such as PDGF β to recruit pericytes, which are critical for tight junction formation. The BBB forms during endothelial cell invasion and pericyte recruitment to the nascent vessels. The evidence has demonstrated that pericytes are not required for induction of BBB-specific genes but are vital to control the relative permeability of CNS during embryogenesis [54, 64]. In early embryogenesis, neural progenitor cells connect with endothelial cells and pericytes to promote BBB maturation. Neural progenitor cells induce angiogenesis and BBB gene expression via the Wnt signaling pathway [54, 57]. Therefore, it is clear that many BBB properties are induced and well formed during early embryogenesis. Another cell type essential for development and maintenance of the BBB is astrocytes. Although astrocytes were first detected in the cerebral cortex at the late embryonic stages around birth, the major differentiation and production of astrocytes occurs during the first month of the postnatal period, suggesting that astrocytes contribute to BBB maturation and maintenance instead of induction of BBB formation [54, 57].

3. hPSC-derived BBB cells

BMECs, pericytes, and astrocytes are the three major cell types forming the BBB and function to tightly regulate the exchange of substances between the blood and the brain tissue. hPSCs could provide

renewable and reproducible sources of these cell types at relatively low costs compared to primary cells. To mimic the *in vivo*-like BBB function, development of reliable and cost-effective differentiation protocols of these cell types is very crucial. Herein, we discuss the representative protocols for BMECs, pericytes, and astrocyte differentiation from PSCs.

3.1 hPSC-derived BMECs

hPSCs, including both hESCs and iPSCs, have previously been differentiated to endothelial cells. PSC-derived BMEC-like cells are identified by expressing tight junction proteins and possessing BBB-like properties, such as low passive permeability, high TEER, and active efflux transporter and RMT functions [66]. The first protocol for differentiation of BMEC-like cells was reported in 2012 [67]. An unconditioned medium (UM) containing Medium/Nutrient Mixture F12 (DMEM/F12), knockout serum replacement, nonessential amino acids, Glutamax, and β -mercaptoethanol was used to initiate co-differentiation to neural and endothelial progenitors within 7 days. The GLUT-1⁺PECAM1⁺ endothelial population is elevated to the predominant cell type by expanding the cells in endothelial cell (EC) medium. Subculture of ECs on fibronectin-collagen type IV matrix is critical for purification and maturation of BMEC-like cells (UM BMEC-like cells). The barrier properties were determined by TEER measurements and active transporter function (Pgp, BCRP, and MRP). Cocultures of UM BMEC-like cells with rodent astrocytes elevated the TEER value from 150-170 $\Omega \cdot \text{cm}^2$ to a maximum of $1,450 \pm 140 \Omega \cdot \text{cm}^2$ and showed expression of a variety of receptors and transporters [67]. During BMEC differentiation, retinoic acid (RA) was shown to trigger several modes of action and boost the passive barrier properties of hPSC-derived BMEC-like cells [68]. RA-treated UM BMEC-like cells (UM-RA BMEC-like cells) exhibited a maximum TEER value of $5350 \pm 250 \Omega \cdot \text{cm}^2$ when cocultured with human primary pericytes and neural progenitor cells in a modified EC medium. However, the TEER value dropped dramatically after 3 days and a large variation was found between UM-RA BMEC-like cells differentiated from different cell lines. The tested function of three efflux transporter families (p-glycoprotein, BCRP, and MRP) increased only MRP expression and activity after RA treatment [68].

E6 medium is a fully-defined and xeno-free medium that was used to replace unconditioned medium to regulate iPSC-derived BMEC-like cell specification by inducing iPSCs to neuroectoderm

[69]. After 4 days treatment with E6 medium, immature BMEC-like cells were switched to human endothelial serum-free medium (hESFM) supplemented with basic fibroblast growth factor (bFGF), RA, and platelet-poor plasma-derived bovine serum (PDS). BMEC-like cells are purified by subculturing cells on fibronectin-collagen type IV matrix with EC medium without bFGF and RA. BMEC-like cells generated with this protocol (E6 BMEC-like cells) have been shown to have equivalent paracellular permeability and efflux transporter activity compared to the UM-based method and maintain TEER values above $1000 \Omega \cdot \text{cm}^2$ for at least 8 days in monoculture [70]. Later, a modified defined protocol arose based on the E6 BMEC-like cells, but replaced PDS with fully defined factors (N2, B27, or ITS) to provide a cost-effective approach to generate BMEC-like cells with more stable TEER values [71]. Neurobasal medium and DMEM/F12 were used to replace the hESFM to study the BBB properties under completely defined culture conditions. The basal media change influenced the gene expression of various transporters and the activity efflux transporter in hPSC-derived BMEC-like cells [72]. In addition to an optimal media composition, the initial cell density of differentiation is crucial for the PSC-derived BMEC-like cells to achieve marked barrier function. For example, in one study, 3.5×10^4 cells/cm² was the optimal seeding density to obtain uniform junction protein expression and high TEER value [73].

Prior to BBB establishment, human brain development in early embryos was purported to occur in a hypoxic environment. Hypoxic conditions have been found to enhance the BBB properties of UM BMEC-like cells, such as ECM deposition, TEER value, and the activity of ABC transporters Pgp, MRP1&4, and BCRP. Hypoxia induced BMEC-like cells also exhibit proper transcellular transport of drugs, peptides, nanoparticle, and antibodies that are dependent on TfR and lipoprotein receptor-related protein. The expression level of Wnt7a also increased 25-fold compared with normoxic conditions [74]. It is important to note that canonical Wnt- β -catenin signaling is necessary for induction of brain angiogenesis. Wnt- β -catenin signaling induces mesodermal and endothelial commitment. Wnt7a and Wnt7b promote BBB specification of UM BMEC-like cells [67]. The canonical Wnt pathway agonist, CHIR99021, directs differentiation of hPSCs to BMEC-like cells through an intermediate primitive streak stage. The subsequent RA treatment leads to BMEC-like cells (CHIR-RA BMEC-like cells) with BBB properties [73]. Notably, RA has been reported to induce endothelial immune quiescence by preventing

the brain endothelium from expressing IL-6, CCL2, and vascular cell adhesion molecules (VCAM) [75]. Similar results showed that UM BMEC-like cells and CHIR-RA BMEC-like cells lack vascular cell adhesion molecules (ICAM-2, VCAM-1, E-selectin, or P-selectin) necessary for immune cell adhesion and trafficking [9]. An extended EC culture method

without RA (EECM) was developed to generate BMEC-like cells (EECM BMEC-like cells). Despite low TEER value and permeability to sodium fluorescein, EECM BMEC-like cells express ICAM-1 and VCAM-1 which increase the Th1 cell adhesion under cytokine stimulated conditions [9].

Table 1. Representative studies for hPSC-derived BMECs

Cell lines	Initial stage	BMEC specification	Markers	Functional assessment	Reference
IMR90-4, DF6-9-9T, DF19-9-11T, H9	Neural and endothelial co-differentiation	UM, hESFM, bFGF, PDS	PECAM-1, Claudin-5, GLUT-1, Pgp, VE-cadherin	TEER: ~850 Ω cm ² LDL uptake Permeability: radiolabeled small molecules Efflux transporter activity: Pgp, MRP, BCRP Tube forming Co-culture with rat astrocytes	[67]
IMR90-4, DF19-9-11T, H9	Neural and endothelial co-differentiation	UM, hESFM, bFGF, PDS, RA	GLUT-1, Claudin-5, Occludin, PECAM-1, VE-cadherin	TEER: ~5000 Ω cm ² Permeability: radiolabeled sucrose Efflux transporter activity: Pgp, MRP, BCRP Tight junction quantification: Occludin, Claudin-5 Co-culture with human primary pericytes, neural progenitor cells, and foreskin fibroblasts	[68]
IMR90-4	Neural and endothelial co-differentiation	UM, hESFM, bFGF, PDS, RA	PECAM-1	OGD induced <i>in vitro</i> model of cerebral ischemia TEER Permeability Cytokine treatment	[80]
CS83iCTR33n1, CS14iCTR28n6, CS21iHD60n8, CS04iHD66n4, CS81iHD71n3, CS09iHD109n1	Neural and endothelial co-differentiation	UM, hESFM, bFGF, PDS, RA	PECAM-1, GLUT-1, Claudin-5, Occludin, ZO-1	TEER: decreased in HD BMEC-like cells Efflux transporter activity: Pgp, ABCB1 Transcytosis: albumin Wound healing assay	[81]
DF19-9-11	Neural and endothelial co-differentiation	UM, hESFM, bFGF, PDS, RA	Claudin-5, Occludin, ZO-1	GBS infection assay TEER	[82]
IMR90-4, DF19-9-11T, H9	Primitive streak-like stage	CHIR99021, bFGF, RA, B27, hESFM,	PECAM-1, ZO-1, VE-cadherin, GLUT-1, Claudin-5, Occludin, BCRP, MRP, Pgp, vWF	TEER: above 3000 Ω cm ² LPL uptake Efflux transporter activity: Pgp, MRP, BCRP Coculture with primary pericytes, hPSC-derived neurons and astrocytes.	[73]
IMR90-4, CD12, SM14, CC3	Neuroectoderm	E6, hESFM, bFGF, PDS, RA	GLUT-1, Claudin-5, Occludin, PECAM-1, VE-cadherin	TEER: above 2500 Ω cm ² Permeability: sodium fluorescein Efflux transporter activity: Pgp, MRP Co-culture with human primary pericytes and iPSC-derived astrocytes	[70]
CC3, CD10, HD70-2, and TSP8-15	Neuroectoderm	E6, hESFM, bFGF, RA, PDS, B27, ITS	PECAM-1, Claudin-5, GLUT-1, VE-cadherin, Occludin	TEER: ~3000 Ω cm ² Permeability: sodium fluorescein Efflux transporter activity: Pgp, MRP Tight junction quantification: Occludin, Claudin-5 Co-culture with human iPSC-derived astrocytes	[71]
IMR90-4	Neural and endothelial co-differentiation	Hypoxia: UM, hESFM, bFGF, PDS, RA	ZO-1, Claudin-5, PECAM-1, GLUT-1, Pgp	TEER: 25000 Ω Efflux transporter activity: Pgp, MRP1, MRP4, BCRP Permeability: 3, 10 kDa dextran	[74]
IMR90-4, H1, H6	Neural and endothelial co-differentiation	UM, hESFM, bFGF, PDS, RA, transduction of <i>FLI1</i> , <i>ERG</i> , and <i>ETV2</i> lentiviral vectors at D6	ZO-1, Occludin, PECAM1, CDH5, EPCAM-1	TEER: ~200 Ω cm ² Permeability: 70 kDa dextran Formation of a capillary network Responses to TNF α	[76]
CC3, CD10, CDH5-2A-eGFP	Neuroectoderm	E6, hESFM, DMEM/F12, neurobasal, bFGF, RA, B27	GLUT-1, Claudin-5, Occludin, VE-cadherin	TEER Permeability: sodium fluorescein Efflux transporter activity: Pgp, MRP	[72]
IMR90-4, iPSC donor 1, 2, and 3.	CD34 ⁺ CD31 ⁺ EC progenitor cells	LaSR, hESFM, B27, bFGF, RA	Claudin-5, Occludin, VE-cadherin, PECAM-1, ZO-1	TEER Permeability: sodium fluorescein Pro-inflammatory cytokine simulation Co-culture with iPSC-derived smooth muscle-like cells, human astrocytes, hiPSC-derived astrocytes, bovine pericytes, and human brain pericytes. Tube forming in mouse	[9]

Notably, hPSC-derived BMEC-like cells differentiated by most current methods lack some phenotypic and functional features of bona fide ECs [76-78]. Transcriptomic analysis has shown underlying epithelial-like gene expression in hPSC-derived BMECs [76, 79]. Recently, there has been a controversy on the identity of PSC-derived BMEC-like cells. Lu, *et al.* employed a comprehensive transcriptomic metanalysis of the hPSC-derived BMEC-like cells generated by current protocols and found that many current protocols produced a homogenous epithelial cell population (including UM [67], UM-RA [68], E6 [70], and defined medium induced BMEC-like cells [71, 73]) lacking vascular endothelial identity [76]. They termed these cells as epi-BMEC-like cells. From their work, overexpression of endothelial ETS factors (ETV2, FLI1, and ERG) in UM induced BMEC-like cells at D6 directs more EC phenotypes. BMECs derived by this method harbor EC transcriptomic profiles, express EC markers (PECAM1, CDH5, KDR), respond to inflammatory stimuli, and display angiogenic properties via tube formation assays in mouse [76].

3.2 hPSC-derived pericytes

The heterogeneous distribution and function of pericytes makes it difficult to accurately distinguish them from other related cell types, such as SMCs or MSCs [83]. No specific markers are known to be unique for their identification. Generally, criteria of multiple markers are applied to isolate and define pericytes; these markers include contractile and cytoskeletal proteins (e.g., desmin, α -smooth muscle actin (α -SMA)) and cell surface antigens (e.g., platelet-derived growth factor receptor β (PDGFR β), transmembrane chondroitin sulfate proteoglycan (NG2), regulator of G-protein signaling-5) [34, 84]. Additionally, these markers also vary within different microvascular zones and developmental stages. Pericytes along the arteriole end of the capillary bed express more α -SMA. In the middle of the capillary bed, pericytes express less α -SMA, and capillary pericytes are α -SMA negative [85, 86]. *In vivo* lineage tracing has revealed that CNS pericytes originate from both mesoderm and ectoderm depending on their exact location. Quail-chick chimera studies have shown that neural crest cells form pericytes in forebrain, while cells of the mesoderm form pericytes in the brainstem, mid-brain, and spinal cord [87, 88]. Lineage tracing in mouse models has shown that capillary pericytes and vascular SMCs in retina, optical nerves and CNS are derived from neural crest [89].

As mesoderm and neural crest are two major origins of pericytes, pericytes have been derived from

hPSCs from both starting points. One approach used embryonic bodies (EBs), cultured in serum through an intermediate multilineage stage containing mesoderm and neuroectoderm. From the EBs, the isolated subset of mesodermal precursors (CD105⁺ CD31⁻ cells) gave rise to CD146⁺NG2⁺PDGFR β ⁺SMA⁻ pericytes [90]. Upon mesoderm to endothelial cell induction, pericytes can be derived from the CD31⁻ fraction by a fully defined protocol [91, 92]. VEGF and SB431542 induce hPSC differentiation toward early vascular cells (EVCs), which can give rise to both endothelial cells and pericytes. Pericytes can be generated from a CD34⁻ population while simultaneously generating endothelial progenitor cells [93]. VEcad⁻ cells sorted from EVCs have the capacity to differentiate to NG2⁺PDGFR β ⁺CD44⁺ pericytes [94, 95].

Meanwhile, coculture of hPSC and OP9 stromal cells induce APLNR⁺PDGFR α ⁺ primitive posterior mesoderm. FGF2 directs APLNR⁺PDGFR α ⁺ primitive posterior mesoderm to mesenchymoblast precursors, which have the potential to generate SMCs, pericytes, and MSCs. Pericytes can be further specified to CD274⁺ capillary and delta like homolog 1 positive arteriolar pericytes, which exhibit a proinflammatory or a contractile phenotype, respectively [96]. Pericytes differentiated from mesoderm are usually found with simultaneous endothelial differentiation. However, neural crest cells were reported to contribute to pericytes and SMCs rather than CNS endothelial cells. Activating Wnt signaling and inhibiting bone morphogenetic protein 4 (BMP4) and activin/nodal signaling induce neural crest stem cell specification. By following culture in a serum contained medium, NSCs can be differentiated to pericytes [97, 98]. Based on these methods, *in vivo* integration, vasculature formation, and co-culture with endothelial cells have been used to confirm pericyte functions (Table 2).

3.3 hPSC-derived astrocytes

Given the significance of astrocytes in CNS function, various protocols have been developed to direct differentiation of hPSCs toward different subtypes of astrocytes (Table 3). Generally, astrocyte differentiation is initiated from an induction of neural progenitor cells, and then followed by astrocyte specification and maturation. Neural progenitor cells (NPCs) are commonly induced in EBs by modulating SMAD signaling pathway [101]. The NPCs in both EB culture or monolayer culture can be initiated and expanded by addition of a cocktail of small molecules (e.g., SB431542, dorsomorphin, noggin) and growth factors (e.g., bFGF, EGF). NPC induction is confirmed by the appearance of neural rosettes and the presence of NPC markers such as Pax6 and Nestin. After neural

induction, astroglial specification is regulated by a combination of various developmental morphogens such as LIF, CNTF, SHH, BMP, and RA. To characterize the hPSC-derived astrocytes, the presence of glial fibrillar acidic protein (GFAP) has been considered as the gold standard for identifying astrocytes. Meanwhile, S100 β is a widely used marker that is expressed in astrocyte progenitors. AQP-4, glutamine synthetase, glutamate transporter-1, and glutamate aspartate transporter (GLAST-1) are also used to identify astrocytes at different stages of differentiation [13]. In addition to specific markers, several assays are available to characterize the functions of hPSC-derived astrocytes. These include analysis of glutamate uptake, calcium signaling, electrophysiological properties, and synapse formation. Promoting the maturation of hPSC-derived astrocytes is challenging due to the heterogeneous morphology and function of astrocyte subtypes in different brain regions. Usually, the protocols for astrocyte differentiation are technically complicated and require long-term culture. The astrocyte yield from these protocols is a mixture of cells at different differentiation stages combined with a lack of regional specification. Recently, hPSC-derived astrocytes show region-specific

phenotypes associated to dorsal and ventral forebrain or dorsal and ventral spinal cord [102].

4. Advances in hPSC-derived BBB modeling

In vitro models that mimic BBB function are crucial tools for studying neurological diseases and developing and testing brain-permeable drugs for clinical use. An ideal BBB model would be fully isogenic from a single source and exhibit robust BBB function with long-term stability. Such a high-fidelity BBB model would increase the efficiency of brain drug screening and boost the development of neurotherapeutics. To date, although reproducing key BBB features *in vitro* remains challenging, many researchers have developed different systems to model the BBB by incorporating hPSC-derived BMEC-like cells, pericytes, astrocytes and neuronal cells (Figure 2). These BBB models have proven useful for studying pathological dysfunction and predicting drug permeability. Thanks to the recent advanced techniques, sensitive and quantitative methods have been established to assess the functions of BBB models.

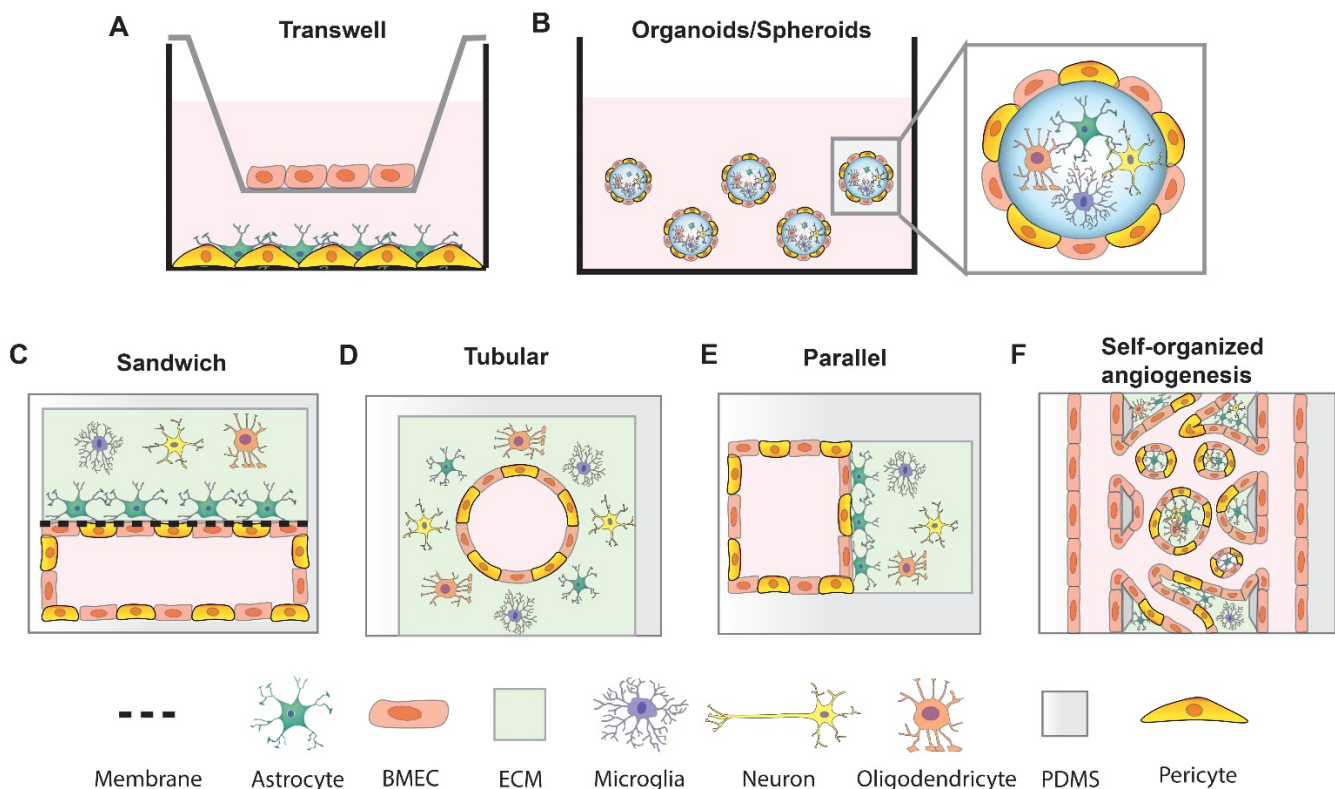


Figure 2. Strategies of *in vitro* BBB models. (A) transwell BBB model; (B) BBB spheroid and organoid model; (C) Sandwich BBB model; (D) Cylindrical tubular BBB model; (E) Parallel BBB model; (F) Self-organized BBB model.

Table 2. Representative studies for hPSC-derived pericytes

Cell lines	Initial stage	Pericytes specification	Markers	Functional assessment	Reference
H9.2, I6, C3, KTR13	Spontaneously differentiated EBs	EBM-2, EC M-19, FBS	CD105, CD90, CD73, CD31, CD146, NG2, and PDGFR	Pericytes and EC assembly Hind limb ischemia model	[90]
H9, H13, clone 26 hCBiPS aMHC ^{neo} PGK ^{hygro} , pCAGGS2, hiPSC-MR31, hESC-H9, hiPSC-BC1	Early vascular cells 12d Pericyte inducing condition 6d	EVC: CIV serum VEGF, SB431542 in EC media Pericytes Serum aMEM	CD73, NG2, PDGFR β , CD44 positive, VE-cadherin and CD31 negative	Self-organized vascular networks in collagen and HA hydrogels <i>In vivo</i> integration	[94, 95]
HESC-NL4, Fib-iPSC	CD31- fraction	Activin A, BMP4, CHIR99021, VEGF, SB43152	PDGFR β , CD146, NG2, CD73, CD44, CD105	Vascular Plexus Zebrafish xenografts	[91] [92]
BOEC-iPSC, NL-HES4, HES3 (NKX2-5eGFP/w)		DMEM, FBS, TGFbeta3, PDGF-BB			
ESI-017	EB	BMP4, FGF2, Activin-A, VEGFA, SB431542	CD146, CD73, and CD105 positive; CD31, CD34, and CD133 negative	Tube formation assay	[99]
H1, H9-EGFP, IISH2i-BM9	Mesenchymal progenitors Immature pericytes	FGF2, PDGF-BB, SB431542, VEGF, EGF	Capillary Phenotype: NG2 ⁺ α -SMA ^{low/-} Desmin ^{low/-} -Calponin ^{low/-} -MYH11- Arteriolar phenotype: NG2 ^{high} α -SMA ⁺ Desmin ⁺ Calponin ^{low/-} -MYH11-	Vasculature formation <i>in vitro</i> and <i>in vivo</i>	[96]
BC1, C12-RFP	Mesoderm, early vascular, pericyte maturation	sB431542, VEGF, pericytes medium	PDGFR β , NG2, CD31, Calponin	Transwell: coculture pericytes with hPSC-derived BMEC-like cells	[100]
AD5, AD6, AD13, AD14, AD20, AD22, AD29, H9 (WA09) and H1 (WA01)	Mesoderm Neural crest	Mesoderm: MIM, DKK1, pericytes medium Neural crest: B27, CHIR99021, pericytes medium	PDGFR β , NG2, CD13, and CD146 positive	Transwell: coculture pericytes with hPSC-derived BMEC-like cells	[97]
H9, IMR90C4, CS03n2	Neural crest	E6, CHIR99021, SB431542, bFGF, dorsomorphin, FBS	PDGFR β , NG2	Self-assembling with endothelial cells Transwell: coculture pericytes with iPSC-derived BMEC-like cells	[98]
H1, H9, DF19-11, 005B23.1, CD3-3, PMBC-3-1, WTC11, WT83, Q83X, M2	Mesoderm CD34- fraction	E8BAC medium: E8, BMP4, Activin-A, and CHIR99021 E7BVi: E8 minus TGF β 1, BMP4, VEGFA, and SB431542	CD34, CD31 negative, PDGFR β , α -SMA, SM22 positive	Angiogenesis assay	[93]

Table 3. Representative studies for hPSC-derived astrocytes

Cell lines	Initial stage	Astrocyte specification	Markers	Functional assessment	References
H9, H7, IMR90-4	Neuroepithelia	RA, FGF8, SHH, CNTF, LIF, FBS	S100 β , GFAP	glutamate uptake synaptogenesis Calcium wave Astrocyte-neuronal co-culture Animal transplantation	[103]
H9, HUES9	bFGF, EGF	B27, BMP4, LIF	S100 β , GFAP, EAAT1, aquaporin	Oxidative neuronal injury	[104]
WA-09, WA-01, IMR90-4, iPSC-Foreskin-1	N2, bFGF, FGF, EGF, CNTF,	N2, CNTF	S100 β , GFAP	Migratory capacity Tropism for hHGG	[105]
H9, H14, BC1	B27, bFGF, CNTF, BMP	CNTF, BMP, FBS	GFAP, TUJ1	Integrate <i>in vivo</i>	[106]
N116213, N117322, 409B2, APP1E111, APP1E211, APP1E311, APP2E22, APP2E26, AD3E211, AD8K213	Cortical neuron: N2, SB431542, dorsomorphin, B27, BDNF, GDNF, NT-3	Repeat passage to a non-coated polystyrene dish	GFAP	Accumulation of Ab oligomers	[107]
4.2 line, GM003814 unaffected 21.8 line, GM002183; SMA 3.6 line, GM003813; SMA 7.12 line, GM09677	bFGF, EGF,	B27, CNTF	GFAP	Disease phenotypes of SMA	[108]
M337V-1, M337V-2, CTRL-1 iPSC line, CTRL-2 iPSC line	LIF, EGF, bFGF,	B27, CNTF	S100 β , GFAP	Astrocyte-neuronal co-culture Disease phenotypes of ALS	[94]
H9, SeV-derived iPSC line and modRNA-derived iPSC line	N2, bFGF, EGF, FGF, CNTF, Noggin, SB431542	CNTF	A2B5, GFAP	<i>In vitro</i> migratory capacity <i>In vivo</i> transplantation	[109]
HC1, HC2, HC3, MS1, MS2, MS3, MS4,	Noggin, bFGF, SB431542	bFGF, EGF, LIF, CNTF	S100 β , GFAP, GLAST	Disease phenotypes of multiple sclerosis	[110]
WA09, H9, RRID:CVCL_9973,GM1-4, RRID:CVCL_7290	N2, B27, SB431542, DMH1	SHH, CHIR99021, CNTF, cyclopamine, prumorphamine, RA, bFGF, BMP4.	Regional markers: S100 β , SOX9, GFAP, HEPACAM.	Basic membrane properties Co-culture with neurons and endothelial cells	[102]

4.1. Functional assessment of BBB models

4.1.1 Junction integrity and coverage

The spatial network of junction proteins in BMECs plays a vital role in stabilizing the BBB function. Immunostaining of both tight junction proteins, such as ZO-1, claudin-5, occludin, and adherins junction proteins, such as VE-cadherin, is commonly used to characterize the barrier integrity of BBB. Disruption of junction proteins revealed by the discontinuous or vanished junction patterns is a characteristic of BBB dysregulation and a hallmark of a number of CNS diseases. Coverage of continuous junction proteins can be quantified to indicate the changes in barrier properties in different conditions. Several methods have been reported to quantify junction integrity. Automated junction analysis by macros or plugins developed with ImageJ have been used to automate and streamline the evaluation of junction organization in cultured cells and the tissue sections [82, 111]. A custom Matlab script was also reported to analyze the junction coverage in iPSC-derived BMEC-like cells [71]. Recently, a Python-based Junction Analyzer Program (JAnaP) was developed by our lab to quantify perimeter junction protein phenotypes along with cell morphological parameters and has been published on GitHub for use by the wider scientific community [112]. Using this program, we have evaluated BMEC junction architecture in response to different matrix stiffnesses, substrate composition, tumor cell-secreted factors, and photodynamic priming for drug delivery applications [112-115]. For 3D vascular structures, a customized UNWRAP application has been developed to convert the cylindrical images to 2D planes [111], and we anticipate that this software can be integrated with the JAnaP to facilitate the quantitative analysis of 3D vessels.

4.1.2 TEER

TEER is a widely accepted quantitative technique for measuring the integrity of tight junctions within a cell monolayer system. In this section, we first introduce the merits of TEER measurements for BBB models, but below we assert concern in utilizing TEER as a gold standard for comparing and assessing these models. The measurement of electrical resistance across a BMEC monolayer can be very sensitive and in general reliably indicates the integrity and permeability of cell monolayers [116]. Conventionally, TEER measurements are performed in a transwell plate in which the BMEC monolayer is cultured on a semipermeable filter insert. The most widely used commercial TEER measurement system is known as

an Epithelial Voltohmmeter that comes equipped with a pair of chopstick electrodes which have been applied in many studies. For electrical measurements, the shorter electrode is placed in the upper insert medium and the longer in the bottom well medium, and so they are separated by the BMEC layer and the transwell mesh support [67, 70]. Compared to the physiological TEER ($1500\text{-}8000\ \Omega\cdot\text{cm}^2$), human primary BMECs have shown limited success in recapitulating the physiological TEER *in vitro*, consistently reporting values below $500\ \Omega\cdot\text{cm}^2$ [1]. Recently, human iPSC-derived BMEC-like cells have been reported to produce TEER values up to $5000\ \Omega\cdot\text{cm}^2$ and show superior junction properties compared with primary BMECs. Coculture of hPSC-derived BMEC-like cells with pericytes, astrocytes or other neural cells can also boost the TEER value and enhance the barrier function. Despite the accepted validity of the TEER readings, in the transwell system, TEER values are not entirely stable, and they are highly dependent on the temperature, medium and electrode position within the wells. To avoid the variation of measurements with the chopstick method, a chamber system with fixed electrode geometry has been developed to generate more uniform results. The above-described systems and values for TEER measurements are mostly confined to static models [89]. However, the physiological shear stress directly influences the barrier function and TEER value. For microfluidic BBB-on-chip systems, the TEER microelectrodes can be directly integrated into the chip system so that the electrodes are inserted to the pre-molded location on each side of the membrane-supported BMEC layer. As a result, TEER measurements can be continuously monitored for long-term study compared to conventional culture systems [117]. Indeed, TEER continues to be a useful tool for measuring cell barrier integrity; however, the BBB community should also carefully consider whether a particular BBB model is also displaying other important BBB phenotypes when evaluating the fidelity of the model.

4.1.3 Permeability

Under physiological conditions, limited permeability of the BBB restricts substances from the blood to the brain, which protects the brain from exposure to molecules that are toxic to the CNS [49]. BBB permeability measurements as a metric for assessing BBB functions are important to understand the disease progression as well as evaluating therapeutic outcomes [118]. Various dyes (e.g. Evans blue, trypan blue), radiolabeled proteins (e.g. albumin), and other markers (e.g. horseradish peroxidase, sucrose, dextran, sodium fluorescein)

have been used to study the permeability of the BBB *in vivo* and *in vitro* and can reflect the different paracellular and transcellular transport mechanisms through the BBB [119]. Fluorescently tagged dextran of varying molecular weights (ranging from 3 to 2,000 kDa) is a commonly used imaging marker for BBB permeability. Because of the wide range of molecular sizes, dextran can be used to test solute, ion, and protein permeability. In short, the fluorescent dextran is applied onto a cell monolayer and allowed to permeate through the cells (via either the paracellular or transcellular pathway), and then flow-through is measured on the other side of the cells (e.g., in a transwell). To precisely capture the integrity of the cell monolayer, small molecules are also available for studies of barrier permeability [120]. Small molecule dyes such as sodium fluorescein (376 Da) and radiolabeled sucrose (342 Da) have been reported to effectively indicate the BBB integrity. With molecular weights of < 500 Da, they may enable detection of more subtle variations in BBB permeability when compared to the use of dextran [119]. Sodium fluorescein and radiolabeled sucrose have been routinely tested on hPSC-derived BMEC-like cells in transwell assays, but they have not been widely used in microfluidic BBB models. Instead, dextran seems to be preferred in microfluidic BBB models. The quantitative measurement of BBB permeability in rodent brain showed that the diffusion values of the small solutes (sodium fluorescein and dextran) were between 3.3×10^{-7} cm/s and 4×10^{-7} cm/s [121, 122]. hPSC-derived BMEC-like cells exhibit high correlation to the *in vivo* brain permeable values [67, 68, 70, 71, 73, 123]. More recently, our lab has used a local permeability assay that was first described by Dubrovskiy *et al* [124] but modified by our lab to incorporate a biotinylated-fibronectin substrate seeded with human BMECs [98], and with FITC-avidin added to the cell culture media. Using this assay, we demonstrated a quantitative correlation between junction phenotype and local permeability [114].

4.1.4 Transporter activity

BBB cells express a broad range of transporters that regulate entry of circulating chemicals into the brain by passive transport, the most well-studied of which are the ABC efflux pumps (Pgp, BCRP, and MRPs) [125]. The most common and effective method to confirm activity of efflux pumps is to perform permeability experiments with inhibitors blocking the function of target efflux pumps in the presence of a specific substrate. For example, Pgp inhibitor (cyclosporin A, tariquidar, reversine, or verapamil) is used to test the Pgp function in BMECs by measuring

the permeability of Rhodamine 123 which is a Pgp substrate. Treatment of Ko143 (a BCRP inhibitor) or MK571 (a MRP family inhibitor) results in increased accumulation of doxorubicin (a BCRP substrate) or 2',7'-dichlorofluorescein diacetate (an MRP family substrate) [67, 68]. The low rate of transcytosis is another important property that maintains the restrictive quality of the BBB. *In vitro* assays of transcytosis have been developed to screen antibodies and ligands and evaluate their therapeutic affinity and capacity [46]. RMT receptors such as low-density lipoprotein receptor-related protein (LRP1), TfR, and insulin receptors abundant in brain capillaries have been exploited to increase the delivery of biotherapeutics to brain [126]. LRP1 has been shown to bind to a variety of ligands such as aprotinin, apolipoprotein E, and lipoprotein lipase etc [127]. Angiopep-2 (ANG) containing 19 amino acids is the well-known ligand to LRP1. Fluorescently labeled ANG has been used to target LRP1 for evaluating the RMT of BBB [128, 129]. Artificial LRP1-binding ligands such as L57 [130] are being researched for LPR-based drug delivery. The iron binding protein, transferrin, is the natural ligand for TfR. Fluorescently labeled transferrin can be used to test the RMT of BBB. Transferrin ligands and antibodies recognizing the TfR have been used for brain targeting [126, 131]. Like the TfR, antibodies capable of binding to insulin receptor have been developed for BBB permeability [126].

4.2 Transwell-based BBB models

Transwell systems are the most commonly used and convenient *in vitro* model for BBB studies (Figure 2A). The low cost, ease of use, wide commercial availability, and flexibility of manipulating experimental conditions makes this apparatus a very robust tool to evaluate BBB properties. In transwell models, endothelial cells are usually cultured on the microporous semi-permeable inserts to form a monolayer on the apical side, while other cell types such as pericytes, astrocytes, or neural progenitor cells are cultured on the lower compartment forming the basolateral side. A range of pore sizes and different membrane compositions are available to satisfy diverse experimental requirements. Transwell-based BBB models with hPSC-derived BMEC monolayers have shown key features of BBB activity such as expression of tight junction proteins, transporter activity, and high TEER values. Incorporating UM-RA BMEC-like cells with pericytes, astrocytes, and NPCs enhances the BBB barrier function [68]. Whole genome expression profiling confirmed the improvement in coculture over a monoculture system [79]. Lippman *et al.* reported that

UM BMEC-like cells cocultured with rodent astrocytes in a transwell system elevated TEER levels for 8 days compared with the TEER from BMEC monolayer, which dramatically decreased within 48 hours [67]. UM-RA BMEC-like cells cocultured with primary human pericytes and neural progenitor cells yielded a significant increase of BMEC monolayer tightness and achieved a TEER value over $5000 \Omega \text{ cm}^2$ [68]. To improve the cell-cell contact, diverse coculture sets with primary or PSC-derived cells have been established based on the transwell system. For example, pericytes and astrocytes have been placed at the bottom surface of the transwell inserts [132]. A 3D printed electrospun poly(lactic-co-glycolic) acid nanofibrous mesh replaced the transwell membrane to remodel the iPSC-derived BMEC and astrocytes interaction [133]. The transwell model is also an important tool to identify matrix compositions and mimic ECM mechanics for BBB formation and maintenance. In another study, biodegradable substrates of varying composition were fine-tuned in a transwell-based BBB model to affect barrier function [134]. Collagen I gel is widely used to prepare hydrogels with low stiffness in BBB models. Coating collagen I hydrogels with basement membrane proteins such as collagen IV, fibronectin, and laminin improves UM-RA BMEC-like cell adhesion and proliferation. In contrast, coating collagen I gels with perlecan leads to poor adhesion of BMECs. Interestingly, although agrin promoted the adhesion of UM-RA BMEC-like cells, the TEER values of iPSC-derived BMEC on agrin-coated membranes were extremely low [134].

Transwell systems can be easily used for permeability screening of molecules or drugs by adding test solute to one side of the porous membrane, and solute concentration is then measured in the opposing well over time. UM-RA BMEC-like cells cultured with hiPSC-derived neural stem cells, pericytes and astrocytes show robust comprehensive transcellular drug transport [132]. Patient-specific isogenic BBB models comprised of iPSC-derived BMEC, pericytes, and astrocytes established using transwell systems provide a valuable platform for neurovascular pathological study and drug discovery [135]. However, this system has several well-known limitations. First, they are 2D monolayer systems that are unable to recapitulate key characteristics of the BBB. BMECs, pericytes, astrocytes or other cell types can only be applied on a flat geometry which lack the complex 3D cell architecture and limit the functionally-relevant cellular contacts. Second, the brain is one of the softest organs in the body. The flat substrates of a transwell membrane are much stiffer than native basement membrane ECM, which

influences the cell-cell and cell-matrix signaling [136]. Although 3D gel transwell systems have been developed to extend the geometry, the limited interaction between cells results in poor BBB properties [134]. In addition, physiological shear stress is missing in this system, which can compromise barrier functions and leads to a model that fails to recapitulate the true *in vivo* environment [137]. Thus, pathophysiological vascular diseases such as cerebral hypoperfusion and ischemia cannot be reproduced in this system.

4.3 Organoid and spheroid BBB models

An organoid is a three-dimensional miniaturized *in vitro* organ that is constructed by pluripotent or adult stem cells from various tissues. BBB organoids consist of multiple cell types that self-assemble in low-adherence culture conditions into multicellular constructs [138]. The cells in BBB organoids and spheroids (Figure 2B) reproduce many BBB features, including high levels of tight junction proteins, an active efflux system, and specific molecular transporters due in part to the wealth of cell-cell contacts in this system [139-142]. The spheroids generated by primary BMECs, pericytes, and astrocytes exhibit higher expression of tight junction proteins, lower paracellular permeability, and higher drug efflux activity compared to a transwell co-culture system [142]. A recently developed cortex organoid model contains six cell types, with BMECs and pericytes encapsulating the organoid generated from iPSC-derived astrocytes, oligodendrocytes, microglia, and neurons. This model recapitulates the various BBB functions and can maintain high cell viability for 21 days [141]. Therefore, an important advantage of iPSC-derived organoid and spheroid models is that multiple cell types can be introduced into this model to more closely recapitulate the intricate NVU. The improved BBB function allows for more understanding of mechanisms of disease modeling and can evaluate the drug action for personalized medicine. However, organoid systems are limited in their size and long-term culture as a result of oxygen diffusion issues into the center of the organoid. The necrotic center has been observed in turn with cerebral organoid maturation [143]. Although a previous study showed a prolonged duration of BBB organoid culture [141], the maintenance of barrier properties is still unclear at these later stages. Moreover, the TEER measurement and incorporation of applied shear stress are challenging in organoid and spheroid models.

4.4 Microfluidic BBB models

The BBB-on-chip systems can mimic the cellular

microenvironment by precisely controlling niche factors such as 3D vessel-like structure, cell-cell interactions, cell-ECM interactions, substrate stiffness, and mechanical shear stress. The microfluidic BBB models that have addressed these characteristics have overcome limitations of other conventional BBB models (transwell or organoids) in aspects of 3D vascular structure and perfusion, live-cell imaging of permeability, and real-time monitoring of TEER value. A number of strategies have been explored to construct microfluidic BBB devices (Table 4, Figure 2C-F).

4.4.1 Microfluidic BBB-on-chip

The classic on-chip model of the capillary comprises two polydimethylsiloxane (PDMS) microchannels which are separated by a porous membrane, giving the overall device the resemblance of a sandwich (Figure 2C). This model has been developed to create a variety of organ models, including (but not limited to) lung [144], gut [145] and BBB. In the BBB models, the porous polycarbonate (PC) membrane is coated with ECM proteins (collagens and fibronectin). BMECs are seeded in the ECM coated channel and brain cells are seeded in the opposite channel. The cells are grown to confluence and fluid flow is introduced into the BMEC compartment to create a blood-brain interface [146, 147]. Usually, in these models, the pore diameter of PC membranes is 0.2 or 0.4 μm and the pore size of PDMS membranes ranges from 0.3 μm to 8 μm . Polyester (PE), polytetrafluoroethylene, and polyethylene terephthalate (PET) membranes have also been reported to support endothelial cells culture in microfluidic devices [74, 148], and these are optically transparent, making it easy to visualize cells by phase contrast microscopy. To assess the barrier function, Ag/AgCl or gold electrodes can be integrated into the chamber layer on opposite sides (blood and brain) of the porous membranes for real-time TEER measurements in the microfluidic system [74, 149]. Wang *et al.* cocultured UM-RA BMEC-like cells with rat primary astrocytes in a BBB-on-chip model with integrated TEER electrodes. This system achieved TEER values above 2000 $\Omega\text{ cm}^2$ for up to 10 days [150]. Vatine *et al.* created a BBB-on-chip with human UM-RA BMEC-like cells and neural progenitors. iPSC-derived neural progenitors supported the BBB maturation with TEER value over 1000 $\Omega\text{ cm}^2$ for 5 days. This system permits whole blood perfusion to the vascular lumen and protects neural cells from blood induced cytotoxicity. Additionally, patient-specific iPSC-derived BBB-on-chip models may predict the drug permeability for drug screenings [151]. However, in these models, the

cell-cell contact is restricted by the pore size and stiffness of membrane and rectangular structure of microchannels. Furthermore, due to the separated channel height, image acquisition in high resolution is challenging.

To mimic realistic vascular geometry, cylindrical tubular microvessels are another popular strategy to fabricate BBB models (Figure 2D). Microvascular tube structures can be constructed by inserting microneedles [152], glass rods [111], or nitinol wire [134, 153] into gel matrix prior to polymerization. After the gel has polymerized, the insert is removed and a cylindrical microchannel remains. Cells can be flowed into the microvessel and allowed to attach and form a monolayer around the sides. This microvessel platform enables controlled blood flow through the BMEC lumen encased by ECM in which pericytes and other neural cells reside to mimic the physiological microvascular structures. These microvessel models have been reported to exhibit robust physiological barrier functions. 150 μm -diameter microvessels were formed by encapsulating iPSC-derived BMEC-like cells in a rat tail type I collagen hydrogel. By crosslinking the matrix with genipin, the stiffness of gels was manipulated, ranging from 0.3-3.3 kPa. Matrix stiffness is well known to affect the adhesion and spreading of BMECs [134]. Although the matrix stiffness did not significantly change the permeability of CHIR-RA BMEC-like cells in microvessels, the dilation response showed an increasing linear trend with increased transmural pressure and a dependence on matrix stiffness [153]. In another study, E6 BMEC-like cells were assembled in a porcine gelatin crosslinked 3D channel and retained stable barrier function (measured by efflux transporter activity) for up to 3 weeks under different shear stresses [154]. In these models, ECM gels can incorporate various cell types to form a biomimetic 3D BBB structure. Cell-cell interactions are more sufficient which facilitate the formation of basement membrane. The stiffness of the ECM can be controlled to mimic the health or disease condition since the stiffness of brain matrix changes in numerous neurological diseases [155-157]. However, it is difficult to integrate the TEER measurements due to the cylindrical structure of these on-chip systems.

Building upon the above noted systems in order to mimic a more complex neurovascular unit, multiple parallel channels have been fabricated to assess the influence of blood vasculature with neural cells in 3D ECM gels (Figure 2E). In one system, ECM gels formed the channel by trapezoidal or phaseguide structures, which can guide the formation of the ECM gel and prevent gel flowing into the adjacent channels [158, 159]. The flanked channel allowed the BMECs to form the blood vessel structure [159]. Based on these

designs, multiple BBB units were integrated into one microfluidic device to facilitate the high-throughput BBB assay. Xu *et al.* created a device that contained 16 independent functional BBB units connected by a microchannel network. Each BBB unit consisted of four BBB regions, each of which consisted of one vascular channel and one parallel channel for ECM collagen or astrocytes [160]. Wevers *et al.* used OrganoPlates, a commercially available microfluidic BBB platform which harbor 40 three-lane or 96 two-lane chips in 384-well plate [161]. These integrated devices make it possible to manipulate shear stress, cell types, nutrient delivery, and drugs to the vascular or brain compartments in a high-throughput manner.

To better recapitulate the physiological features of the BBB, self-organized microvascular networks were generated to mimic the natural processes of angiogenesis [162] (Figure 2F). Endothelial cells sprout from preexisting vascular channels and self-assemble into tubular structures in adjacent ECM

gels [163, 164]. The resulting microvessels form intact and perfusable capillaries and exhibit native physiological morphologies. This BBB model allows for high-resolution imaging of key events at the BBB, such as cancer cell extravasation [165]. Incorporation of pericytes and astrocytes assists the ECs in forming smaller (diameters ranging from 10 to 50 μm) and more branched vascular networks with decreased permeability values and upregulated BBB transporters [166]. One limitation of this model is the difficulty to integrate the TEER measurement; however, we reiterate that TEER is likely not the best method for assessing and comparing BBB models. An additional limitation is that the fibrinogen hydrogel commonly used in this self-assembly model does not fully recapitulate the brain ECM. Meanwhile, the ability to continuously perfuse fluid through these model microvascular networks is an attractive feature and should be incorporated in more future studies [167].

Table 4: Representative studies for hPSC-derived microfluidic BBB-on-chip

Cell lines	Seed cells	Fluidic channel	Shear stress	Matrix	BBB markers	Function	Time of observation	Reference
BC1	UM BMEC-like cells	four rectangular channels with different heights	4 and 12 dyne/cm ²	Collagen IV, Fibronectin	Occludin Claudin-5 F-actin ZO-1	Cell morphology, proliferation, apoptosis, protein gene expression under shear stress	40 h	[168]
IMR-90-4	UM-RA BMEC-like cells, Rat primary astrocytes	Neuronal Chamber: 6.5 mm diameter Microchannels: 300 μm width \times 160 μm height PC membrane: 0.4 μm diameter pores TEER electrode	0.023-1.8 dyne/cm ²	Collagen IV, Fibronectin	Claudin-5, ZO-1	TEER: 2000-4000 Ω cm ² Permeability: 4, 20, 70 kDa Dextran, caffeine, cimetidine, doxorubicin	10 days	[150]
BC1	UM-RA BMEC-like cells	Diameter: 150 μm	0.1, 1 dyne/cm ²	Collagen I Laminin/entactin, Genipin, Collagen IV, Fibronectin	ZO-1, Claudin-5	TEER: transwell Permeability: 70 kDa Dextran	3 days	[134]
CS0617iCTR, CS0172 iCTR, CS0188 iCTR, CS81iHD, CS03iCTR, CS03iCTR ^{mut} , CS01iMCT8, CS01iMCT8 ^{cor}	UM-RA BMEC-like cells, primary pericytes and astrocytes	Brain channel: 1 \times 1 mm Blood channel: 1 \times 0.2 mm PDMS membrane: 7 μm diameter pores	0.01, 0.5, 2.4, 5 dyne/cm ²	Collagen IV, Fibronectin	Occludin Claudin-5 ZO-1, PECAM-1, GLUT-1	TEER Permeability: 3, 4, 20, 70 kDa Dextran T3, IgG, Albumin, Transferrin Efflux transporter activity: Pgp Viability: LDH	10 days	[151]
IMR90-4	Hypoxia induced UM-RA BMEC-like cells, human primary pericytes, and astrocytes	Brain channel: 2cm long \times 1mm wide \times 1mm high Blood channel: 2cm long \times 1mm wide \times 0.2 mm high PET membranes Pore size: 0.4 μm	6 dyne/cm ²	Collagen IV, Fibronectin	ZO-1, Claudin-5, PECAM-1, GLUT-1, Pgp	TEER: 25000 Ω Efflux transporter activity: Pgp, MRP1, MRP4, BCRP Permeability: 3, 10 kDa dextran	2 weeks	[74]
BC1-GFP, C12-RFP	CHIR-RA BMEC-like cells	Diameter: 150 μm	1 dyne/cm ²	Collagen I, Genipin, Matrigel	ZO-1	Permeability: Lucifer yellow, 10 kDa dextran	2 days	[153]
IMR90-4, CC3	E6 BMEC-like cells, HUVEC, μVas	Diameter: 800 μm	0.3, 1, 3 dyne/cm ²	Gelatin	Occludin Claudin-5 VE-cadherin F-actin	Permeability: 3 kDa Dextran, Albumin Efflux transporter activity: Pgp, MRP	21 days	[154]
	iPSC-ECs, human primary pericytes, and astrocytes	Self-organized vessels Diameter: 10-200 μm	Not identified	Fibrin gel	ZO-1, Occludin Claudin-5	Permeability: 10 kDa and 40 kDa dextran	7 days	[166]

4.4.2 Shear stress in microfluidic BBB models

Shear stress is generated by blood flow and acts tangentially on the endothelial surface of blood vessels. Shear stress is a key mechanical cue that is critical in maintaining a stable BBB phenotype. Shear stress not only alters cellular morphology and differentiation of BMECs but can also trigger biochemical and biological events [169]. In the BBB, BMECs regulate the transport of solutes and water between blood and brain tissues by sensing the shear stress. The physiological shear stresses range from 1-4 dyn/cm² in venous systems to 10-20 dyn/cm² in capillaries [168]. Physiological shear stress applications result in an elongated spindle-like morphology and alignment of peripheral endothelial cells in the direction of flow. In contrast to peripheral endothelial cells, primary BMECs resist elongation and alignment in response to shear stress and maintain their cobblestone-like morphology [111, 170]. Consistent with primary BMECs, iPSC-derived BMEC-like cells do not elongate and align upon exposure to shear stress [168]. Meanwhile, shear stress decreased the proliferation, apoptosis, and cell displacement of iPSC-derived BMEC-like cells but did not affect the expression of key BBB markers in a microfluidic model [168]. Shear stress enhances the integrity and stabilizes the barrier function of iPSC-derived BMEC-like cells. Several BBB models demonstrated that shear stress increased the TEER value [150, 151]. A recent microfluidic system achieved physiological relevant TEER values by coculturing UM-RA BMEC-like cells with iPSC-derived neural progenitors [151]. In a perfused hydrogel model, E6 BMEC-like cells were 10-100 times less permeable than HUVECs and primary BMECs. E6 BMEC-like cells exposed to shear stress (1 and 3.2 dyn/cm²) for 14 days that went through angiogenic sprouting and reduction of passive barrier function displayed a measured permeability value much lower than E6 BMEC-like cells cultured in static conditions [154]. Physiologic shear stress protects the BMECs from inflammatory cytokines, while abnormal flow patterns impair barrier function of BMECs. Meanwhile, loss of flow induced TNF- α release, which decreased the expression of occludin, claudin-5, and VE-cadherin in BMECs and increased BBB permeability [171, 172]. However, high shear stress (40 dyn/cm²) or pulsatility also decreased the expression of tight junction markers [173]. Thus, maintaining the shear forces at physiologically relevant conditions is very important to stabilize BBB function.

5. BBB disease modeling

BBB dysfunction has been observed as a feature of various neurological diseases, including PD, AD, Huntington's disease (HD), and amyotrophic lateral sclerosis (ALS) [174]. hiPSCs could be harnessed as powerful tools to recreate functional NVUs which provide a promising route to reconstruct functional BBBs *in vitro*. Beyond mimicking BBB physiological function, isogenic and patient-customized models have great promise to replicate complex disease processes such as progression of neurological diseases, brain metastases, and CNS infections. These applications also lend themselves useful for drug screening for novel treatments of these brain diseases. A cerebral ischemia model was created with iPSC-derived BMEC-like cells by inducing an oxygen-glucose deprivation (OGD) condition. TNF α was found to prevent the restoration of barrier integrity in OGD induced ischemia [80]. E6 BMEC-like cells from patients with genetic neurological diseases show compromised barrier functions; for example, they carry mutations in PARK2, a PD early onset gene, which leads to loss of Pgp function in an apical-basolateral transport assay [70]. Familial AD mutations (presenilin1 and presenilin2) display impaired barrier properties and glucose metabolism which are associated with the β -amyloid (A β) deposition in AD iPSC-derived BMEC-like cells [175, 176]. Also, apolipoprotein (APOE4) is the strongest risk factor for sporadic AD. APOE4/4 iPSC-derived CHIR-RA BMEC-like cells, pericytes, and astrocytes self-assembled in Matrigel, forming capillary-like structures. APOE4 BBB models show AD vascular pathology upon increased A β accumulation, which is attributed to the dysregulation of nuclear factor of activated T cells-calcineurin signaling in APOE4/4 iPSC-derived pericytes [177]. Additionally, UM-RA BMEC-like cells of HD patients manifest cell-autonomous deficits including impaired MDR1 function, transcytosis, and altered gene networks of barrier and angiogenesis [81]. The expression of junction protein (Claudin-5) and TEER values were also significantly decreased in BMEC-like cells derived from iPSCs of HD patients [71]. The monocarboxylate transporter 8 (MCT8)-deficient UM-RA BMEC-like cells derived from iPSCs of psychomotor retardation patients exhibited no significant differences in TEER and fluorescein permeability but showed reduced triiodothyronine (T3) permeability. The restoration of T3 transport can be explored as a potential to screen for drugs to treat MCT8-deficient patients [178].

Microfluidic BBB-on-chips permit the recreation of multicellular BBB architectures by incorporating multiple iPSC-derived cells. Personalized

BBB-on-chips incorporating iPSC-derived UM-RA BMEC-like cells, astrocytes, and neurons exhibited physiological relevance with low paracellular permeability, high TEER value, response to inflammatory cues (IL-1 β , IL-8, TNF- α), active transferrin RMT, and efflux transport. BBB chips from MCT8 HD and psychomotor retardation patients treated with whole human blood perfusion mimic multiple disease features and can be used to predict CNS drug penetrability [151]. Meanwhile, a recent study showed that a BBB-on-chip allowed for more rapid evaluation of nanoparticle permeability, which could potentially predict nanoparticle transport and contribute to screening of nanotherapeutics [179]. In addition, CRISPR/Cas9-mediated genome editing in patient-derived iPSCs allows for precise therapies targeted to inherited neurological diseases. Correction of mutants in HD and MCT-8-deficient iPSCs restores the barrier function in BBB models [153]. In brain metastasis, malignant tumor cells have the ability to transmigrate through the BMECs of brain capillaries to enter into brain. Lung cancer, breast cancer, and malignant melanoma contribute to the majority of brain metastases [180]. A high-throughput BBB-on-chip reproduced the process of tumor cell extravasation across the BBB by perfusing various cancer cell types through the vascular compartment [160]. Lastly, to date, the exact mechanism of how the pathogens such as viruses and bacteria cross the BBB and enter the CNS is still largely unknown. Kim *et al.* showed that group B *Streptococcus* (GBS) invaded UM BMEC-like cells and activated cells to upregulate the proinflammatory chemokines and cytokines which contribute to the disruption of the tight junction components [82]. Thus, iPSC-derived BBB models could uncover the infection process of pathogens within CNS.

6. Challenges and perspective

Thanks to the advances in human PSC-based technologies, a series of brain cell types derived from PSCs have been able to pave the way for superior BBB modeling. Significant efforts have been made to reconstruct BBB structure in 2D or 3D models which have incorporated the typical BBB features and have been utilized for various applications such as disease modeling, drug screening, and personalized medicine. Microfluidic BBB-on-chip models show huge potential to recapitulate more complex structure and function of *in vivo* BBB than conventional 2D BBB models which provide a more promising tool to facilitate mechanobiological study and drug discovery. Moreover, BBB models established from healthy or diseased donors could lead to more effective personalized therapies or novel drugs.

Although PSC-derived BBB models have developed rapidly, their clinical applications are still at an early stage.

The ideal BBB model should reproduce the sophisticated brain structures and function which involve multiple determining factors such as cell invasion and migration, cell-cell interaction, controllable fluidic flow, and biomimetic microenvironment. The major challenges of BBB modeling are gaps between the *in vitro* model and *in vivo* capillary structure. Human brain perforating capillaries (the most abundant type) can be as small as 5-8 μm in diameter, and the inter-capillary distance is around 40-60 μm [21, 181]. Most current approaches for modeling the BBB in microfluidic devices involve creating microchannels around 75-100 μm , which is closer to the size of arterioles or post-capillary venules [1]. Self-assembled microvessels can achieve smaller capillaries with diameters of around 25-30 μm [166].

The BBB traits are generated by a dynamic interplay with multiple cell types including BMECs, pericytes, astrocytes and other neural cells. Primary BMECs lose their superior barrier properties when cultured *in vitro*. The current hPSC-derived BBB models are dependent upon the heterogeneous incorporation of hPSC-derived BMECs, pericytes and astrocytes. hPSC-derived BMEC-like cells recapitulate many functional and molecular features of *in vivo* BMECs and significantly improve our understanding of BBB development and functions [66]. However, restricted by the differentiation methods, many models lack some phenotypic and functional aspects of *in vivo* BMECs, such as the key adhesion molecules involved in immune cell migration, some transporter activity, and responses to inflammatory stimuli [9, 74]. Transcriptomic analysis highlights that epithelial-like genes are expressed in the hPSC-derived BMEC-like cells. It has been suggested that the most current protocols for BMECs differentiation produce a more homogenous epithelial cell population instead of endothelial cells [76, 79]. Although transcriptomic profiles may not fully match the proteome expressed in BMECs, these results raise the questions of whether the epi-BMEC-like cells are suitable for use as *in vitro* BBB models and if these models are physiologically relevant and predictive of the *in vivo* situation. Meanwhile, many studies support that the hPSC-derived BMECs possess multiple of the requisite BBB markers and phenotypes, such as strong barrier properties, and a new model even captures relevant immune phenotypes [66]. Continued efforts are required to develop homogenous BMECs for stable and reliable BBB models.

Although hPSC-derived BMECs, pericytes and

astrocytes are usually included in BBB models *in vitro*, cells derived from different protocols are not well evaluated in the BBB models. How cell origins, such as hPSC mesoderm- or neuroectoderm-derived BMECs and pericytes affect the function of BBB models is still under-researched. Beyond assembling BMECs, pericytes, and astrocytes together, a combination of other NVU cell types, such as neural cells, may contribute to more comprehensive microenvironments and functionality of BBB models. Generally, neurological diseases exhibit brain vascular pathologies associated with changes in different brain regions, which may lead to different neuro-pathologies [40]. The current iPSC-derived BBB models are simple assemblies of vascular associated cells and neuronal cells in different channels or gels without forming sophisticated 3D structures specific to particular brain regions. Region-specific BBB-associated pericytes, astrocytes, and neuronal cells have not been fully identified. Even in the current simplified BBB models, the direct and/or paracrine interaction of different cell types is still under-researched. It is important to note that hPSC-derived microglia or oligodendrocytes are missing in most of the current BBB model constructions which may have further effects on BBB function. The microfluidic BBB vasculature combined with cerebral organoids in a 3D manner may give more insights into these questions [182]. In addition, age-related shifts in BBB dysfunction allow neurotoxic proteins to enter the aged parenchyma, which can trigger neuroinflammation and provoke neurodegenerative disease. Using iPSC-derived cells to recapitulate the BBB in an aging brain is still proving to be a challenge. Furthermore, recent work has identified that sex of cells is an important biological parameter that impacts neurodegenerative disease and BBB integrity, though most studies fail to address these discrepancies [183]. Hence, comprehensive studies are still necessary to develop *in vitro* models that fully reflect the physiological functions of the BBB, such as the exchange of molecules, cell trafficking, and immune responses in different scenarios (age, sex, or disease-related conditions).

The mechanical cues from underlying matrix have been documented to influence the BBB properties [184]. A range of materials (collagen I, collagen IV, fibronectin, laminin, and agrin, etc.) have been explored with the aim of reproducing physical cues for the BBB *in vitro*. However, incorporation of multiple characteristics (cell-cell interaction, cell-matrix interaction, physiological shear stress, etc.) in 3D BBB models remains challenging. The materials with lower Young's Moduli, high pore densities, and

the capability of recapitulating sophisticated 3D structure and interactions of the BBB are highly desired [185]. In addition, long-term maintenance of BBB properties under dynamic fluid flow is still a challenge. Flow-mediated shear stress can promote the barrier properties of BBB models. The long-term culture of BBB models will be necessary for the study of chronic and age-associated diseases such as multiple sclerosis, PD or AD. So far, the longest successful culture of a microfluidic PSC-derived BBB model is around 3 weeks [154]. The barrier function decreased over time which was also associated with different shear stresses applied to the flow system. Moreover, in most cases, the fluidic flow is perfused by culture medium, whereas whole blood perfusion could better mimic the *in vivo* physiological scenario. The optimized cultured condition is crucial to maintain a long-term culture. How to stabilize the barrier properties under a wide range of physiological blood flows still needs to be determined in the future studies. Furthermore, to meet the needs of the pharmaceutical industry, *in vitro* BBB systems should be stable, fully scalable, high throughput, and customizable with high predictability and reproducibility. These will require the incorporation of a number of automations such as real-time monitoring and control of physiological parameters, medium sampling, and data analysis, which will greatly minimize variability and facilitate operator efforts.

Despite significant advances in generating various hPSC-derived NVU cells and engineering novel BBB models, it is still challenging to incorporate all the relevant factors such as different NVU cells, ECM, and mechanical cues in one BBB model. The complexities and the limitation of different BBB models need to consider for the goals of the experiments. One needs to keep in mind that the reduced complexities of the BBB modeling would not fully recapitulate the function of BBB and compromise the outcomes. Therefore, the field should be continuing to work towards generating the full experimental insights that could be used to identify, in a systematic way, what *in vitro* model characteristics are sufficient to generate informative and relevant data.

Abbreviations

ABC: ATP-binding cassette; AD: Alzheimer's disease; ALS: amyotrophic lateral sclerosis; ANG: angiotensin-converting enzyme 2; BBB: blood-brain barrier; BCRP: breast cancer resistance protein; BDNF: brain-derived neurotrophic factor; bFGF: basic fibroblast growth factor 2; BMECs: brain microvascular endothelial cells; BMP: Bone morphogenetic protein; CNS: central

neuron system; CDH5: cadherin 5; CNTF: ciliary neurotrophic factor; DMH1: dorsomorphin homologue 1; EB: embryo body; EBM-2: endothelial cell growth basal medium-2; ECs: endothelial cells; ECM: extracellular matrix; EGF: epidermal growth factor;; EPCAM: epithelial cell adhesion molecule; ERG: E-twenty six-related gene; EGF: epidermal growth factor; ETV2: E-twenty six variant 2; FBS: fetal bovine serum; FL1: friend leukemia integration 1 transcription factor; GDNF: glial cell line-derived neurotrophic factor; GFAP: glial fibrillary acidic protein; GLAST: glutamate transporter; GBS: *Streptococcus agalactiae*; GLUT-1: Glucose transporter 1; HA: hyaluronic acid; HD: Huntington's disease; hESC: human embryonic stem cell; hESFM: human endothelial serum-free medium; hHGG: human high-grade gliomas; ICAMs: leukocyte adhesion molecules; iPSC: induced pluripotent stem cells; ITS: insulin, transferrin, and selenium; LDL: low-density lipoprotein; LIF: leukemia inhibitory factor; LPR1: low-density lipoprotein receptor-related protein; MIM: mesoderm induction medium; MRP: multidrug resistance associated protein; MSC: mesenchymal stem cells; NPCs: neural progenitor cells; NT-3: neurotrophin-3; OGD: oxygen-glucose deprivation; PC: polycarbonate; PET: polyethylene terephthalate; PSC: pluripotent stem cell; NVU: neurovascular unit; PDGF-BB: platelet-derived growth factor-BB; PDS: platelet-poor plasma-derived serum; PECAM-1 (CD31): platelet endothelial cell adhesion molecule-1; Pgp: P-glycoproteins; RA: retinoic acid; RMT: receptor mediated transcytosis; RMT: receptor mediated transcytosis; SHH: sonic hedgehog; SMA: spinal muscular atrophy; TfR: transferrin receptor; TGF: transforming growth factor; TNF α : tumor necrosis factor alpha; VEGF: vascular endothelial growth factor; ZO-1: zonula occluden-1.

Acknowledgements

The authors gratefully acknowledge support from a Maryland Stem Cell Research Fund Discovery Grant.

Author Contributions

LY, RM, and KMS wrote and edited the manuscript. All authors read and approved the final manuscript.

Competing Interests

The authors have declared that no competing interest exists.

References

- DeStefano JG, Jamieson JJ, Linville RM, Searson PC. Benchmarking in vitro tissue-engineered blood-brain barrier models. *Fluids Barriers CNS*. 2018; 15: 32.
- Choi JH, Santhosh M, Choi JW. In Vitro Blood-Brain Barrier-Integrated Neurological Disorder Models Using a Microfluidic Device. *Micromachines* (Basel). 2019; 11: 21.
- Pardridge WM. Drug transport across the blood-brain barrier. *J Cereb Blood Flow Metab*. 2012; 32: 1959-72.
- Pamies D, Hartung T, Hogberg HT. Biological and medical applications of a brain-on-a-chip. *Exp Biol Med* (Maywood). 2014; 239: 1096-107.
- Ghose AK, Viswanadhan VN, Wendoloski JJ. A knowledge-based approach in designing combinatorial or medicinal chemistry libraries for drug discovery. 1. A qualitative and quantitative characterization of known drug databases. *J Comb Chem*. 1999; 1: 55-68.
- van der Helm MW, van der Meer AD, Eijkel JC, van den Berg A, Segerink LI. Microfluidic organ-on-chip technology for blood-brain barrier research. *Tissue Barriers*. 2016; 4: e1142493.
- Georgieva JV, Goulatis LI, Stutz CC, Canfield SG, Song HW, Gastfriend BD, et al. Antibody screening using a human iPSC-based blood-brain barrier model identifies antibodies that accumulate in the CNS. *FASEB J*. 2020; 34: 12549-64.
- Jamieson JJ, Searson PC, Gerecht S. Engineering the human blood-brain barrier in vitro. *J Biol Eng*. 2017; 11: 37.
- Nishihara H, Gastfriend BD, Soldati S, Perriot S, Mathias A, Sano Y, et al. Advancing human induced pluripotent stem cell-derived blood-brain barrier models for studying immune cell interactions. *FASEB J*. 2020; 34: 16693-715.
- Jeske R, Albo J, Marzano M, Bejoy J, Li Y. Engineering Brain-Specific Pericytes from Human Pluripotent Stem Cells. *Tissue Eng Part B Rev*. 2020; 26: 367-82.
- Yan L, Jiang B, Li E, Wang X, Ling Q, Zheng D, et al. Scalable Generation of Mesenchymal Stem Cells from Human Embryonic Stem Cells in 3D. *Int J Biol Sci*. 2018; 14: 1196-210.
- Jiang B, Yan L, Wang X, Li E, Murphy K, Vaccaro K, et al. Concise Review: Mesenchymal Stem Cells Derived from Human Pluripotent Cells, an Unlimited and Quality-Controllable Source, for Therapeutic Applications. *Stem Cells*. 2019; 37:572-81.
- Chandrasekaran A, Avci HX, Leist M, Kobolak J, Dinnyes A. Astrocyte Differentiation of Human Pluripotent Stem Cells: New Tools for Neurological Disorder Research. *Front Cell Neurosci*. 2016; 10: 215.
- Lippmann ES, Al-Ahmad A, Palecek SP, Shusta EV. Modeling the blood-brain barrier using stem cell sources. *Fluids Barriers CNS*. 2013; 10: 2.
- Yan L, Jiang B, Niu Y, Wang H, Li E, Yan Y, et al. Intrathecal delivery of human ESC-derived mesenchymal stem cell spheres promotes recovery of a primate multiple sclerosis model. *Cell Death Discov*. 2018; 4: 28.
- Tian X, Brookes O, Battaglia G. Pericytes from Mesenchymal Stem Cells as a model for the blood-brain barrier. *Sci Rep*. 2017; 7: 39676.
- Lauschke K, Frederiksen L, Hall VJ. Paving the Way Toward Complex Blood-Brain Barrier Models Using Pluripotent Stem Cells. *Stem Cells Dev*. 2017; 26: 857-74.
- Aday S, Cecchelli R, Hallier-Vanuxeem D, Dehouck MP, Ferreira L. Stem Cell-Based Human Blood-Brain Barrier Models for Drug Discovery and Delivery. *Trends Biotechnol*. 2016; 34: 382-93.
- Jiang L, Li S, Zheng J, Li Y, Huang H. Recent Progress in Microfluidic Models of the Blood-Brain Barrier. *Micromachines* (Basel). 2019; 10: 375.
- Cassot F, Lauwers F, Fouard C, Prohaska S, Lauwers-Cances V. A novel three-dimensional computer-assisted method for a quantitative study of microvascular networks of the human cerebral cortex. *Microcirculation*. 2006; 13: 1-18.
- Wong AD, Ye M, Levy AF, Rothstein JD, Bergles DE, Searson PC. The blood-brain barrier: an engineering perspective. *Front Neuroeng*. 2013; 6: 7.
- Greene C, Campbell M. Tight junction modulation of the blood brain barrier: CNS delivery of small molecules. *Tissue Barriers*. 2016; 4: e1138017.
- Wolburg H, Lippoldt A. Tight junctions of the blood-brain barrier: development, composition and regulation. *Vascul Pharmacol*. 2002; 38: 323-37.
- Campbell HK, Maiers JL, DeMali KA. Interplay between tight junctions & adherens junctions. *Exp Cell Res*. 2017; 358: 39-44.
- Haseloff RF, Dithmer S, Winkler L, Wolburg H, Blasig IE. Transmembrane proteins of the tight junctions at the blood-brain barrier: structural and functional aspects. *Semin Cell Dev Biol*. 2015; 38: 16-25.
- Engelhardt B, Liebner S. Novel insights into the development and maintenance of the blood-brain barrier. *Cell Tissue Res*. 2014; 355: 687-99.
- Zhao Y, Xin Y, He Z, Hu W. Function of Connexins in the Interaction between Glial and Vascular Cells in the Central Nervous System and Related Neurological Diseases. *Neural Plast*. 2018; 2018: 6323901.
- Evans WH, De Vuyst E, Leybaert L. The gap junction cellular internet: connexin hemichannels enter the signalling limelight. *Biochem J*. 2006; 397: 1-14.
- Butt AM, Jones HC, Abbott NJ. Electrical resistance across the blood-brain barrier in anaesthetized rats: a developmental study. *J Physiol*. 1990; 429: 47-62.
- Mathiesen TM, Lehre KP, Danbolt NC, Ottersen OP. The perivascular astroglial sheath provides a complete covering of the brain microvessels: an electron microscopic 3D reconstruction. *Glia*. 2010; 58: 1094-103.
- Armulik A, Genove G, Mae M, Nisancioglu MH, Wallgard E, Niaudet C, et al. Pericytes regulate the blood-brain barrier. *Nature*. 2010; 468: 557-61.
- Bonkowski D, Katyshev V, Balabanov RD, Borisov A, Dore-Duffy P. The CNS microvascular pericyte: pericyte-astrocyte crosstalk in the regulation of tissue survival. *Fluids Barriers CNS*. 2011; 8: 8.

33. Yao Y, Chen ZL, Norris EH, Strickland S. Astrocytic laminin regulates pericyte differentiation and maintains blood brain barrier integrity. *Nat Commun.* 2014; 5: 3413.
34. Sweeney MD, Ayyadurai S, Zlokovic BV. Pericytes of the neurovascular unit: key functions and signaling pathways. *Nat Neurosci.* 2016; 19: 771-83.
35. Vasile F, Dossi E, Rouach N. Human astrocytes: structure and functions in the healthy brain. *Brain Struct Funct.* 2017; 222: 2017-29.
36. Camassa LMA, Lunde LK, Hoddevik EH, Stensland M, Boldt HB, De Souza GA, et al. Mechanisms underlying AQP4 accumulation in astrocyte endfeet. *Glia.* 2015; 63: 2073-91.
37. Siracusa R, Fusco R, Cuzzocrea S. Astrocytes: Role and Functions in Brain Pathologies. *Front Pharmacol.* 2019; 10: 1114.
38. Jang E, Kim JH, Lee S, Kim JH, Seo JW, Jin M, et al. Phenotypic polarization of activated astrocytes: the critical role of lipocalin-2 in the classical inflammatory activation of astrocytes. *J Immunol.* 2013; 191: 5204-19.
39. Sofroniew MV. Astrocyte barriers to neurotoxic inflammation. *Nat Rev Neurosci.* 2015; 16: 249-63.
40. Villabona-Rueda A, Erice C, Pardo CA, Stins MF. The Evolving Concept of the Blood Brain Barrier (BBB): From a Single Static Barrier to a Heterogeneous and Dynamic Relay Center. *Front Cell Neurosci.* 2019; 13: 405.
41. Baeten KM, Akassoglou K. Extracellular matrix and matrix receptors in blood-brain barrier formation and stroke. *Dev Neurobiol.* 2011; 71: 1018-39.
42. Daneman R, Prat A. The blood-brain barrier. *Cold Spring Harb Perspect Biol.* 2015; 7: a020412.
43. Sweeney MD, Zhao Z, Montagne A, Nelson AR, Zlokovic BV. Blood-Brain Barrier: From Physiology to Disease and Back. *Physiol Rev.* 2019; 99: 21-78.
44. Abbott NJ, Patabendige AA, Dolman DE, Yusof SR, Begley DJ. Structure and function of the blood-brain barrier. *Neurobiol Dis.* 2010; 37: 13-25.
45. Patching SG. Glucose Transporters at the Blood-Brain Barrier: Function, Regulation and Gateways for Drug Delivery. *Mol Neurobiol.* 2017; 54: 1046-77.
46. Pulgar VM. Transcytosis to Cross the Blood Brain Barrier, New Advancements and Challenges. *Front Neurosci.* 2018; 12: 1019.
47. Zhang W, Liu QY, Haqqani AS, Leclerc S, Liu Z, Fauteux F, et al. Differential expression of receptors mediating receptor-mediated transcytosis (RMT) in brain microvessels, brain parenchyma and peripheral tissues of the mouse and the human. *Fluids Barriers CNS.* 2020; 17: 47.
48. Loscher W, Potschka H. Blood-brain barrier active efflux transporters: ATP-binding cassette gene family. *NeuroRx.* 2005; 2: 86-98.
49. Saunders NR, Dreifuss JJ, Dziegielewska KM, Johansson PA, Habgood MD, Mollgard K, et al. The rights and wrongs of blood-brain barrier permeability studies: a walk through 100 years of history. *Front Neurosci.* 2014; 8: 404.
50. Saunders NR, Liddelow SA, Dziegielewska KM. Barrier mechanisms in the developing brain. *Front Pharmacol.* 2012; 3: 46.
51. Grazer FM, Clemente CD. Developing blood brain barrier to trypan blue. *Proc Soc Exp Biol Med.* 1957; 94: 758-60.
52. Olsson Y, Klatzo I, Sourander P, Steinwall O. Blood-brain barrier to albumin in embryonic new born and adult rats. *Acta Neuropathol.* 1968; 10: 117-22.
53. Saunders NR, Dziegielewska KM, Mollgard K, Habgood MD. Recent Developments in Understanding Barrier Mechanisms in the Developing Brain: Drugs and Drug Transporters in Pregnancy, Susceptibility or Protection in the Fetal Brain? *Annu Rev Pharmacol Toxicol.* 2019; 59: 487-505.
54. Daneman R, Zhou L, Kebede AA, Barres BA. Pericytes are required for blood-brain barrier integrity during embryogenesis. *Nature.* 2010; 468: 562-6.
55. Urayama A, Grubb JH, Sly WS, Banks WA. Mannose 6-phosphate receptor-mediated transport of sulfamidase across the blood-brain barrier in the newborn mouse. *Mol Ther.* 2008; 16: 1261-6.
56. Tata M, Ruhrberg C, Fantin A. Vascularisation of the central nervous system. *Mech Dev.* 2015; 138 Pt 1: 26-36.
57. Blanchette M, Daneman R. Formation and maintenance of the BBB. *Mech Dev.* 2015; 138 Pt 1: 8-16.
58. Obermeier B, Daneman R, Ransohoff RM. Development, maintenance and disruption of the blood-brain barrier. *Nat Med.* 2013; 19: 1584-96.
59. Dermietzel R, Krause D, Kremer M, Wang C, Stevenson B. Pattern of glucose transporter (Glut 1) expression in embryonic brains is related to maturation of blood-brain barrier tightness. *Dev Dyn.* 1992; 193: 152-63.
60. Strazielle N, Ghersi-Egea JF. Efflux transporters in blood-brain interfaces of the developing brain. *Front Neurosci.* 2015; 9: 21.
61. Kniessel U, Risau W, Wolburg H. Development of blood-brain barrier tight junctions in the rat cortex. *Brain Res Dev Brain Res.* 1996; 96: 229-40.
62. Stewart PA, Hayakawa K. Early ultrastructural changes in blood-brain barrier vessels of the rat embryo. *Brain Res Dev Brain Res.* 1994; 78: 25-34.
63. Alvarez JL, Dodelet-Devillers A, Kebir H, Ifergan I, Fabre PJ, Terouz S, et al. The Hedgehog pathway promotes blood-brain barrier integrity and CNS immune quiescence. *Science.* 2011; 334: 1727-31.
64. Ben-Zvi A, Lacoste B, Kur E, Andreone BJ, Mayshar Y, Yan H, et al. Mfsd2a is critical for the formation and function of the blood-brain barrier. *Nature.* 2014; 509: 507-11.
65. Virgintino D, Errede M, Robertson D, Capobianco C, Girolamo F, Vimercati A, et al. Immunolocalization of tight junction proteins in the adult and developing human brain. *Histochem Cell Biol.* 2004; 122: 51-9.
66. Lippmann ES, Azarin SM, Palecek SP, Shusta EV. Commentary on human pluripotent stem cell-based blood-brain barrier models. *Fluids Barriers CNS.* 2020; 17: 64.
67. Lippmann ES, Azarin SM, Kay JE, Nessler RA, Wilson HK, Al-Ahmad A, et al. Derivation of blood-brain barrier endothelial cells from human pluripotent stem cells. *Nat Biotechnol.* 2012; 30: 783-91.
68. Lippmann ES, Al-Ahmad A, Azarin SM, Palecek SP, Shusta EV. A retinoic acid-enhanced, multicellular human blood-brain barrier model derived from stem cell sources. *Sci Rep.* 2014; 4: 4160.
69. Lippmann ES, Estevez-Silva MC, Ashton RS. Defined human pluripotent stem cell culture enables highly efficient neuroepithelium derivation without small molecule inhibitors. *Stem Cells.* 2014; 32: 1032-42.
70. Hollmann EK, Bailey AK, Potharazu AV, Neely MD, Bowman AB, Lippmann ES. Accelerated differentiation of human induced pluripotent stem cells to blood-brain barrier endothelial cells. *Fluids Barriers CNS.* 2017; 14: 9.
71. Neal EH, Marinelli NA, Shi Y, McClatchey PM, Balotin KM, Gullett DR, et al. A Simplified, Fully Defined Differentiation Scheme for Producing Blood-Brain Barrier Endothelial Cells from Human iPSCs. *Stem Cell Reports.* 2019; 12: 1380-8.
72. Emma H, Neal KAK, Yajuan Shi, Nicholas A, Marinelli, Kameron A, Hagerla, Ethan S, Lippmann. Influence of basal media composition on barrier fidelity within human pluripotent stem cell-derived blood-brain barrier models. *bioRxiv.* 2021.
73. Qian T, Maguire SE, Canfield SG, Bao X, Olson WR, Shusta EV, et al. Directed differentiation of human pluripotent stem cells to blood-brain barrier endothelial cells. *Sci Adv.* 2017; 3: e1701679.
74. Park TE, Mustafaoglu N, Herland A, Hasselkus R, Mannix R, FitzGerald EA, et al. Hypoxia-enhanced Blood-Brain Barrier Chip recapitulates human barrier function and shuttling of drugs and antibodies. *Nat Commun.* 2019; 10: 2621.
75. Mizze MR, Nijland PG, van der Pol SM, Drexhage JA, van Het Hof B, Mebius R, et al. Astrocyte-derived retinoic acid: a novel regulator of blood-brain barrier function in multiple sclerosis. *Acta Neuropathol.* 2014; 128: 691-703.
76. Lu TM, Houghton S, Magdeldin T, Duran JGB, Minotti AP, Snead A, et al. Pluripotent stem cell-derived epithelium misidentified as brain microvascular endothelium requires ETS factors to acquire vascular fate. *Proc Natl Acad Sci U S A.* 2021; 118: e2016950118.
77. Lu TM, Barcia Duran JG, Houghton S, Rafii S, Redmond D, Lis R. Human Induced Pluripotent Stem Cell-Derived Brain Endothelial Cells: Current Controversies. *Front Physiol.* 2021; 12: 642812.
78. Workman MJ, Svendsen CN. Recent advances in human iPSC-derived models of the blood-brain barrier. *Fluids Barriers CNS.* 2020; 17: 30.
79. Delsing L, Donnes P, Sanchez J, Clausen M, Voulgaris D, Falk A, et al. Barrier Properties and Transcriptome Expression in Human iPSC-Derived Models of the Blood-Brain Barrier. *Stem Cells.* 2018; 36: 1816-27.
80. Kokubu Y, Yamaguchi T, Kawabata K. In vitro model of cerebral ischemia by using brain microvascular endothelial cells derived from human induced pluripotent stem cells. *Biochem Biophys Res Commun.* 2017; 486: 577-83.
81. Lim RG, Quan C, Reyes-Ortiz AM, Lutz SE, Kedaigle AJ, Gipson TA, et al. Huntington's Disease iPSC-Derived Brain Microvascular Endothelial Cells Reveal WNT-Mediated Angiogenic and Blood-Brain Barrier Deficits. *Cell Rep.* 2017; 19: 1365-77.
82. Kim BJ, Bee OB, McDonagh MA, Stebbins MJ, Palecek SP, Doran KS, et al. Modeling Group B Streptococcus and Blood-Brain Barrier Interaction by Using Induced Pluripotent Stem Cell-Derived Brain Endothelial Cells. *mSphere.* 2017; 2: e00398-17.
83. Steeland S, Van Ryckeghem S, Van Imschoot G, De Rycke R, Toussaint W, Vanhoutte L, et al. TNFR1 inhibition with a Nanobody protects against EAE development in mice. *Sci Rep.* 2017; 7: 13646.
84. Xu J, Gong T, Heng BC, Zhang CF. A systematic review: differentiation of stem cells into functional pericytes. *FASEB J.* 2017; 31: 1775-86.
85. Bandopadhyay R, Orte C, Lawrenson JG, Reid AR, De Silva S, Allt G. Contractile proteins in pericytes at the blood-brain and blood-retinal barriers. *J Neurocytol.* 2001; 30: 35-44.
86. Alarcon-Martinez L, Yilmaz-Ozcan S, Yemisci M, Schallek J, Kilic K, Can A, et al. Capillary pericytes express alpha-smooth muscle actin, which requires prevention of filamentous-actin depolymerization for detection. *Elife.* 2018; 7: e34861.
87. Etchevers HC, Vincent C, Le Douarin NM, Couly GF. The cephalic neural crest provides pericytes and smooth muscle cells to all blood vessels of the face and forebrain. *Development.* 2001; 128: 1059-68.
88. Korn J, Christ B, Kurz H. Neuroectodermal origin of brain pericytes and vascular smooth muscle cells. *J Comp Neurol.* 2002; 442: 78-88.
89. Trost A, Schroedl F, Lange S, Rivera FJ, Tempfer H, Korntner S, et al. Neural crest origin of retinal and choroidal pericytes. *Invest Ophthalmol Vis Sci.* 2013; 54: 7910-21.
90. Dar A, Domev H, Ben-Yosef O, Tzukerman M, Zeevi-Levin N, Novak A, et al. Multipotent vasculogenic pericytes from human pluripotent stem cells promote recovery of murine ischemic limb. *Circulation.* 2012; 125: 87-99.
91. Orlova VV, Drabsch Y, Freund C, Petrus-Reurer S, van den Hil FE, Muenthaingon S, et al. Functionality of endothelial cells and pericytes from human pluripotent stem cells demonstrated in cultured vascular plexus and zebrafish xenografts. *Arterioscler Thromb Vasc Biol.* 2014; 34: 177-86.
92. Orlova VV, van den Hil FE, Petrus-Reurer S, Drabsch Y, Ten Dijke P, Mummery CL. Generation, expansion and functional analysis of endothelial cells and pericytes derived from human pluripotent stem cells. *Nat Protoc.* 2014; 9: 1514-31.

93. Zhang J, Schwartz MP, Hou Z, Bai Y, Ardalani H, Swanson S, et al. A Genome-wide Analysis of Human Pluripotent Stem Cell-Derived Endothelial Cells in 2D or 3D Culture. *Stem Cell Reports*. 2017; 8: 907-18.
94. Serio A, Bilican B, Barnada SJ, Ando DM, Zhao C, Siller R, et al. Astrocyte pathology and the absence of non-cell autonomy in an induced pluripotent stem cell model of TDP-43 proteinopathy. *Proc Natl Acad Sci U S A*. 2013; 110: 4697-702.
95. Wanjare M, Kusuma S, Gerecht S. Defining Differences among Perivascular Cells Derived from Human Pluripotent Stem Cells. *Stem Cell Reports*. 2014; 2: 746.
96. Kumar A, D'Souza SS, Moskvina OV, Toh H, Wang B, Zhang J, et al. Specification and Diversification of Pericytes and Smooth Muscle Cells from Mesenchymal Stem Cells. *Cell Rep*. 2017; 19: 1902-16.
97. Faal T, Phan DTT, Davtyan H, Scarfone VM, Varady E, Blurton-Jones M, et al. Induction of Mesoderm and Neural Crest-Derived Pericytes from Human Pluripotent Stem Cells to Study Blood-Brain Barrier Interactions. *Stem Cell Reports*. 2019; 12: 451-60.
98. Stebbins MJ, Gastfriend BD, Canfield SG, Lee MS, Richards D, Faubion MG, et al. Human pluripotent stem cell-derived brain pericyte-like cells induce blood-brain barrier properties. *Sci Adv*. 2019; 5: eaau7375.
99. Greenwood-Goodwin M, Yang J, Hassanipour M, Larocca D. A novel lineage restricted, pericyte-like cell line isolated from human embryonic stem cells. *Sci Rep*. 2016; 6: 24403.
100. Jamieson JJ, Linville RM, Ding YY, Gerecht S, Searson PC. Role of iPSC-derived pericytes on barrier function of iPSC-derived brain microvascular endothelial cells in 2D and 3D. *Fluids Barriers CNS*. 2019; 16: 15.
101. Tyzack G, Lakatos A, Patani R. Human Stem Cell-Derived Astrocytes: Specification and Relevance for Neurological Disorders. *Curr Stem Cell Rep*. 2016; 2: 236-47.
102. Bradley RA, Shireman J, McFalls C, Choi J, Canfield SG, Dong Y, et al. Regionally specified human pluripotent stem cell-derived astrocytes exhibit different molecular signatures and functional properties. *Development*. 2019; 146: dev170910.
103. Krencik R, Weick JP, Liu Y, Zhang ZJ, Zhang SC. Specification of transplantable astroglial subtypes from human pluripotent stem cells. *Nat Biotechnol*. 2011; 29: 528-34.
104. Gupta K, Patani R, Baxter P, Serio A, Story D, Tsujita T, et al. Human embryonic stem cell derived astrocytes mediate non-cell-autonomous neuroprotection through endogenous and drug-induced mechanisms. *Cell Death Differ*. 2012; 19: 779-87.
105. Emdad L, D'Souza SL, Kothari HP, Qadeer ZA, Germano IM. Efficient differentiation of human embryonic and induced pluripotent stem cells into functional astrocytes. *Stem Cells Dev*. 2012; 21: 404-10.
106. Shaltouki A, Peng J, Liu Q, Rao MS, Zeng X. Efficient generation of astrocytes from human pluripotent stem cells in defined conditions. *Stem Cells*. 2013; 31: 941-52.
107. Kondo T, Asai M, Tsukita K, Kutoku Y, Ohsawa Y, Sunada Y, et al. Modeling Alzheimer's disease with iPSCs reveals stress phenotypes associated with intracellular Abeta and differential drug responsiveness. *Cell Stem Cell*. 2013; 12: 487-96.
108. McGivern JV, Patitucci TN, Nord JA, Barabas MA, Stucky CL, Ebert AD. Spinal muscular atrophy astrocytes exhibit abnormal calcium regulation and reduced growth factor production. *Glia*. 2013; 61: 1418-28.
109. Mormone E, D'Souza S, Alexeeva V, Bederson MM, Germano IM. "Footprint-free" human induced pluripotent stem cell-derived astrocytes for in vivo cell-based therapy. *Stem Cells Dev*. 2014; 23: 2626-36.
110. Perriot S, Mathias A, Perriard G, Canales M, Jonkmans N, Merienne N, et al. Human Induced Pluripotent Stem Cell-Derived Astrocytes Are Differentially Activated by Multiple Sclerosis-Associated Cytokines. *Stem Cell Reports*. 2018; 11: 1199-210.
111. Ye M, Sanchez HM, Hultz M, Yang Z, Bogorad M, Wong AD, et al. Brain microvascular endothelial cells resist elongation due to curvature and shear stress. *Sci Rep*. 2014; 4: 4681.
112. Gray KM, Katz DB, Brown EG, Stroka KM. Quantitative Phenotyping of Cell-Cell Junctions to Evaluate ZO-1 Presentation in Brain Endothelial Cells. *Ann Biomed Eng*. 2019; 47: 1675-87.
113. Ingult CT, Gray KM, Vig S, Jung JW, Stabile J, Zhang Y, et al. Photodynamic Priming Modulates Endothelial Cell-Cell Junction Phenotype for Light-activated Remote Control of Drug Delivery. *IEEE J Sel Top Quantum Electron*. 2021; 27: 7200311.
114. Gray KM, Jung JW, Ingult CT, Huang HC, Stroka KM. Quantitatively relating brain endothelial cell-cell junction phenotype to global and local barrier properties under varied culture conditions via the Junction Analyzer Program. *Fluids Barriers CNS*. 2020; 17: 16.
115. Pranda MA, Gray KM, DeCastro AJL, Dawson GM, Jung JW, Stroka KM. Tumor Cell Mechanosensing During Incorporation into the Brain Microvascular Endothelium. *Cell Mol Bioeng*. 2019; 12: 455-80.
116. Srinivasan B, Kolli AR, Esch MB, Abaci HE, Shuler ML, Hickman JJ. TEER measurement techniques for in vitro barrier model systems. *J Lab Autom*. 2015; 20: 107-26.
117. Henry OYF, Villenave R, Cronce MJ, Leineweber WD, Benz MA, Ingber DE. Organs-on-chips with integrated electrodes for trans-epithelial electrical resistance (TEER) measurements of human epithelial barrier function. *Lab Chip*. 2017; 17: 2264-71.
118. Chowdhury EA, Noorani B, Alqahtani F, Bhalerao A, Raut S, Sivandzade F, et al. Understanding the brain uptake and permeability of small molecules through the BBB: A technical overview. *J Cereb Blood Flow Metab*. 2021; 41: 1797-820.
119. Saunders NR, Dziegielewska KM, Mollgard K, Habgood MD. Markers for blood-brain barrier integrity: how appropriate is Evans blue in the twenty-first century and what are the alternatives? *Front Neurosci*. 2015; 9: 385.
120. Oddo A, Peng B, Tong Z, Wei Y, Tong WY, Thissen H, et al. Advances in Microfluidic Blood-Brain Barrier (BBB) Models. *Trends Biotechnol*. 2019; 37: 1295-314.
121. Shi L, Zeng M, Sun Y, Fu BM. Quantification of blood-brain barrier solute permeability and brain transport by multiphoton microscopy. *J Biomech Eng*. 2014; 136: 031005.
122. Deosarkar SP, Prabhakarapandian B, Wang B, Sheffield JB, Krynska B, Kiani MF. A Novel Dynamic Neonatal Blood-Brain Barrier on a Chip. *PLoS One*. 2015; 10: e0142725.
123. Roux GL, Jarray R, Guyot AC, Pavoni S, Costa N, Theodoro F, et al. Proof-of-Concept Study of Drug Brain Permeability Between in Vivo Human Brain and an in Vitro iPSCs-Human Blood-Brain Barrier Model. *Sci Rep*. 2019; 9: 16310.
124. Dubrovskiy O, Birukova AA, Birukov KG. Measurement of local permeability at subcellular level in cell models of agonist- and ventilator-induced lung injury. *Lab Invest*. 2013; 93: 254-63.
125. Qosa H, Miller DS, Pasinelli P, Trotti D. Regulation of ABC efflux transporters at blood-brain barrier in health and neurological disorders. *Brain Res*. 2015; 1628: 298-316.
126. Terstappen GC, Meyer AH, Bell RD, Zhang W. Strategies for delivering therapeutics across the blood-brain barrier. *Nat Rev Drug Discov*. 2021; 20: 362-83.
127. Lillis AP, Van Duyn LB, Murphy-Ullrich JE, Strickland DK. LDL receptor-related protein 1: unique tissue-specific functions revealed by selective gene knockout studies. *Physiol Rev*. 2008; 88: 887-918.
128. Demeule M, Currie JC, Bertrand Y, Che C, Nguyen T, Regina A, et al. Involvement of the low-density lipoprotein receptor-related protein in the transcytosis of the brain delivery vector angiopep-2. *J Neurochem*. 2008; 106: 1534-44.
129. Ji X, Wang H, Chen Y, Zhou J, Liu Y. Recombinant expressing angiopep-2 fused anti-VEGF single chain Fab (scFab) could cross blood-brain barrier and target glioma. *AMB Express*. 2019; 9: 165.
130. Sakamoto K, Shinohara T, Adachi Y, Asami T, Ohtaki T. A novel LRP1-binding peptide L57 that crosses the blood brain barrier. *Biochem Biophys Res Commun*. 2017; 12: 135-9.
131. Jones AR, Shusta EV. Blood-brain barrier transport of therapeutics via receptor-mediated. *Pharm Res*. 2007; 24: 1759-71.
132. Appelt-Menzel A, Cubukova A, Gunther K, Edenhofer F, Piontek J, Krause G, et al. Establishment of a Human Blood-Brain Barrier Co-culture Model Mimicking the Neurovascular Unit Using Induced Pluri- and Multipotent Stem Cells. *Stem Cell Reports*. 2017; 8: 894-906.
133. Qi D, Wu S, Lin H, Kuss MA, Lei Y, Krasnoslobodtsev A, et al. Establishment of a Human iPSC- and Nanofiber-Based Microphysiological Blood-Brain Barrier System. *ACS Appl Mater Interfaces*. 2018; 10: 21825-35.
134. Katt ME, Linville RM, Mayo LN, Xu ZS, Searson PC. Functional brain-specific microvessels from iPSC-derived human brain microvascular endothelial cells: the role of matrix composition on monolayer formation. *Fluids Barriers CNS*. 2018; 15: 7.
135. Canfield SG, Stebbins MJ, Morales BS, Asai SW, Vatine GD, Svendsen CN, et al. An isogenic blood-brain barrier model comprising brain endothelial cells, astrocytes, and neurons derived from human induced pluripotent stem cells. *J Neurochem*. 2017; 140: 874-88.
136. Janmey PA, Fletcher DA, Reinhart-King CA. Stiffness Sensing by Cells. *Physiol Rev*. 2020; 100: 695-724.
137. Ruck T, Bittner S, Meuth SG. Blood-brain barrier modeling: challenges and perspectives. *Neural Regen Res*. 2015; 10: 889-91.
138. Urich E, Patsch C, Aigner S, Graf M, Iacone R, Freskgard PO. Multicellular self-assembled spheroidal model of the blood brain barrier. *Sci Rep*. 2013; 3: 1500.
139. Benjamin EJ, Virani SS, Callaway CW, Chamberlain AM, Chang AR, Cheng S, et al. Heart Disease and Stroke Statistics-2018 Update: A Report From the American Heart Association. *Circulation*. 2018; 137: e67-e492.
140. Bhalerao A, Sivandzade F, Archie SR, Chowdhury EA, Noorani B, Cuccullo L. In vitro modeling of the neurovascular unit: advances in the field. *Fluids Barriers CNS*. 2020; 17: 22.
141. Nzou G, Wicks RT, Wicks EE, Seale SA, Sane CH, Chen A, et al. Human Cortex Spheroid with a Functional Blood Brain Barrier for High-Throughput Neurotoxicity Screening and Disease Modeling. *Sci Rep*. 2018; 8: 7413.
142. Cho CF, Wolfe JM, Fadzen CM, Calligaris D, Hornburg K, Chiocca EA, et al. Blood-brain-barrier spheroids as an in vitro screening platform for brain-penetrating agents. *Nat Commun*. 2017; 8: 15623.
143. Grebenyuk S, Ranga A. Engineering Organoid Vascularization. *Front Bioeng Biotechnol*. 2019; 7: 39.
144. Huh D, Matthews BD, Mammoto A, Montoya-Zavala M, Hsin HY, Ingber DE. Reconstituting organ-level lung functions on a chip. *Science*. 2010; 328: 1662-8.
145. Huh D, Kim HJ, Fraser JP, Shea DE, Khan M, Bahinski A, et al. Microfabrication of human organs-on-chips. *Nat Protoc*. 2013; 8: 2135-57.

146. Booth R, Kim H. Characterization of a microfluidic in vitro model of the blood-brain barrier (muBBB). *Lab Chip*. 2012; 12: 1784-92.
147. Achyuta AK, Conway AJ, Crouse RB, Bannister EC, Lee RN, Katnik CP, et al. A modular approach to create a neurovascular unit-on-a-chip. *Lab Chip*. 2013; 13: 542-53.
148. Sellgren KL, Hawkins BT, Grego S. An optically transparent membrane supports shear stress studies in a three-dimensional microfluidic neurovascular unit model. *Biomicrofluidics*. 2015; 9: 061102.
149. Wang JD, Khafagy el S, Khanafer K, Takayama S, ElSayed ME. Organization of Endothelial Cells, Pericytes, and Astrocytes into a 3D Microfluidic in Vitro Model of the Blood-Brain Barrier. *Mol Pharm*. 2016; 13: 895-906.
150. Wang YI, Abaci HE, Shuler ML. Microfluidic blood-brain barrier model provides in vivo-like barrier properties for drug permeability screening. *Biotechnol Bioeng*. 2017; 114: 184-94.
151. Vatine GD, Barrile R, Workman MJ, Sances S, Barriga BK, Rahnama M, et al. Human iPSC-Derived Blood-Brain Barrier Chips Enable Disease Modeling and Personalized Medicine Applications. *Cell Stem Cell*. 2019; 24: 995-1005 e6.
152. Polacheck WJ, Kutys ML, Tefft JB, Chen CS. Microfabricated blood vessels for modeling the vascular transport barrier. *Nat Protoc*. 2019; 14: 1425-54.
153. Grifino GN, Farrell AM, Linville RM, Arevalo D, Kim JH, Gu L, et al. Tissue-engineered blood-brain barrier models via directed differentiation of human induced pluripotent stem cells. *Sci Rep*. 2019; 9: 13957.
154. Faley SL, Neal EH, Wang JX, Bosworth AM, Weber CM, Balotin KM, et al. iPSC-Derived Brain Endothelium Exhibits Stable, Long-Term Barrier Function in Perfused Hydrogel Scaffolds. *Stem Cell Reports*. 2019; 12: 474-87.
155. Hiscox LV, Johnson CL, McGarry MDJ, Marshall H, Ritchie CW, van Beek EJR, et al. Mechanical property alterations across the cerebral cortex due to Alzheimer's disease. *Brain Commun*. 2020; 2: fcz049.
156. Hall CM, Moendarbary E, Sheridan GK. Mechanobiology of the brain in ageing and Alzheimer's disease. *Eur J Neurosci*. 2020; 53: 3851-78.
157. Barnes JM, Przybyla L, Weaver VM. Tissue mechanics regulate brain development, homeostasis and disease. *J Cell Sci*. 2017; 130: 71-82.
158. Shin Y, Yang K, Han S, Park HJ, Seok Heo Y, Cho SW, et al. Reconstituting vascular microenvironment of neural stem cell niche in three-dimensional extracellular matrix. *Adv Healthc Mater*. 2014; 3: 1457-64.
159. Adriani G, Ma D, Pavesi A, Kamm RD, Goh EL. A 3D neurovascular microfluidic model consisting of neurons, astrocytes and cerebral endothelial cells as a blood-brain barrier. *Lab Chip*. 2017; 17: 448-59.
160. Xu H, Li Z, Yu Y, Sizdahkhani S, Ho WS, Yin F, et al. A dynamic in vivo-like organotypic blood-brain barrier model to probe metastatic brain tumors. *Sci Rep*. 2016; 6: 36670.
161. Wevers NR, Kasi DG, Gray T, Wilschut KJ, Smith B, van Vught R, et al. A perfused human blood-brain barrier on-a-chip for high-throughput assessment of barrier function and antibody transport. *Fluids Barriers CNS*. 2018; 15: 23.
162. Bang S, Lee SR, Ko J, Son K, Tahk D, Ahn J, et al. A Low Permeability Microfluidic Blood-Brain Barrier Platform with Direct Contact between Perfusable Vascular Network and Astrocytes. *Sci Rep*. 2017; 7: 8083.
163. Shin Y, Han S, Jeon JS, Yamamoto K, Zervantonakis IK, Sudo R, et al. Microfluidic assay for simultaneous culture of multiple cell types on surfaces or within hydrogels. *Nat Protoc*. 2012; 7: 1247-59.
164. Chung S, Sudo R, Mack PJ, Wan CR, Vickerman V, Kamm RD. Cell migration into scaffolds under co-culture conditions in a microfluidic platform. *Lab Chip*. 2009; 9: 269-75.
165. Chen MB, Whisler JA, Frose J, Yu C, Shin Y, Kamm RD. On-chip human microvasculature assay for visualization and quantification of tumor cell extravasation dynamics. *Nat Protoc*. 2017; 12: 865-80.
166. Campisi M, Shin Y, Osaki T, Hajal C, Chiono V, Kamm RD. 3D self-organized microvascular model of the human blood-brain barrier with endothelial cells, pericytes and astrocytes. *Biomaterials*. 2018; 180: 117-29.
167. Hajal C, Le Roi B, Kamm RD, Maoz BM. Biology and Models of the Blood-Brain Barrier. *Annu Rev Biomed Eng*. 2021; 23: 359-84.
168. DeStefano JG, Xu ZS, Williams AJ, Yimam N, Searson PC. Effect of shear stress on iPSC-derived human brain microvascular endothelial cells (dhBMECs). *Fluids Barriers CNS*. 2017; 14: 20.
169. Wang X, Xu B, Xiang M, Yang X, Liu Y, Liu X, et al. Advances on fluid shear stress regulating blood-brain barrier. *Microvasc Res*. 2020; 128: 103930.
170. Reintz A, DeStefano J, Ye M, Wong AD, Searson PC. Human brain microvascular endothelial cells resist elongation due to shear stress. *Microvasc Res*. 2015; 99: 8-18.
171. Krizanac-Bengez L, Mayberg MR, Cunningham E, Hossain M, Ponnampalam S, Parkinson FE, et al. Loss of shear stress induces leukocyte-mediated cytokine release and blood-brain barrier failure in dynamic in vitro blood-brain barrier model. *J Cell Physiol*. 2006; 206: 68-77.
172. Rochfort KD, Collins LE, McLoughlin A, Cummins PM. Shear-dependent attenuation of cellular ROS levels can suppress proinflammatory cytokine injury to human brain microvascular endothelial barrier properties. *J Cereb Blood Flow Metab*. 2015; 35: 1648-56.
173. Garcia-Polite F, Martorell J, Del Rey-Puech P, Melgar-Lesmes P, O'Brien CC, Roquer J, et al. Pulsatility and high shear stress deteriorate barrier phenotype in brain microvascular endothelium. *J Cereb Blood Flow Metab*. 2017; 37: 2614-25.
174. Profaci CP, Munji RN, Pulido RS, Daneman R. The blood-brain barrier in health and disease: Important unanswered questions. *J Exp Med*. 2020; 217: e20190062.
175. Oikari LE, Pandit R, Stewart R, Cuni-Lopez C, Quek H, Sutharsan R, et al. Altered Brain Endothelial Cell Phenotype from a Familial Alzheimer Mutation and Its Potential Implications for Amyloid Clearance and Drug Delivery. *Stem Cell Reports*. 2020; 14: 924-39.
176. Katt ME, Mayo LN, Ellis SE, Mahairaki V, Rothstein JD, Cheng L, et al. The role of mutations associated with familial neurodegenerative disorders on blood-brain barrier function in an iPSC model. *Fluids Barriers CNS*. 2019; 16: 20.
177. Blanchard JW, Bula M, Davila-Velderrain J, Akay LA, Zhu L, Frank A, et al. Reconstruction of the human blood-brain barrier in vitro reveals a pathogenic mechanism of APOE4 in pericytes. *Nat Med*. 2020; 26: 952-63.
178. Vatine GD, Al-Ahmad A, Barriga BK, Svendsen S, Salim A, Garcia L, et al. Modeling Psychomotor Retardation using iPSCs from MCT8-Deficient Patients Indicates a Prominent Role for the Blood-Brain Barrier. *Cell Stem Cell*. 2017; 20: 831-43 e5.
179. Lee S, Chung M, Lee SR, Jeon NL. 3D brain angiogenesis model to reconstitute functional human blood-brain barrier in vitro. *Biotechnol Bioeng*. 2020; 117: 748-62.
180. Krizbai IA, Gasparics A, Nagyoszi P, Fazakas C, Molnar J, Wilhelm I, et al. Endothelial-mesenchymal transition of brain endothelial cells: possible role during metastatic extravasation. *PLoS One*. 2015; 10: e0123845.
181. Marin-Padilla M. The human brain intracerebral microvascular system: development and structure. *Front Neuroanat*. 2012; 6: 38.
182. Wang Y, Wang L, Zhu Y, Qin J. Human brain organoid-on-a-chip to model prenatal nicotine exposure. *Lab Chip*. 2018; 18: 851-60.
183. Weber CM, Clyne AM. Sex differences in the blood-brain barrier and neurodegenerative diseases. *APL Bioeng*. 2021; 5: 011509.
184. Gray KM, Stroka KM. Vascular endothelial cell mechanosensing: New insights gained from biomimetic microfluidic models. *Semin Cell Dev Biol*. 2017; 71: 106-17.
185. Ferro MP, Heilshorn SC, Owens RM. Materials for blood brain barrier modeling in vitro. *Mater Sci Eng R Rep*. 2020; 140: 100522.

Author Biography



Dr. Li Yan is currently an Assistant Research Professor in the Fischell Department of Bioengineering at the University of Maryland. She received her Ph.D. in Biochemistry and Molecular Biology at China Agricultural University. After completing her Ph.D., she joined Yunnan Key Laboratory of Primate Medical Research Center as a research fellow. She then carried out her postdoctoral research at the University of Macau, on stem cell therapies in the Faculty of Health Science. Dr. Yan is the author of 20 articles. Her research interests include stem cell differentiation, stem cell therapies, disease modeling with genome editing, and blood-brain barrier engineering.



Dr. **Kimberly M. Stroka** is an Associate Professor in the Fischell Department of Bioengineering at the University of Maryland, College Park. Dr. Stroka received a B.S. degree in physics from Denison University (Granville, OH, USA) a Ph.D. degree in bioengineering from the University of Maryland, College Park. From 2012 to 2014, she was a Postdoctoral Fellow with the Institute for NanoBioTechnology at The Johns Hopkins University (Baltimore, MD, USA). Dr. Stroka is the author of 39 articles and 3 book chapters. Her research interests include cell mechanobiology, cell mechanics, cell-cell interactions, cell-substrate interactions, cell migration, blood-brain barrier modeling, and microfabricated devices for modeling of cellular systems. Dr. Stroka is a member of the Biomedical Engineering Society. She is the recipient of the NSF Graduate Research Fellowship, NIH F31 and F32 Fellowships, Burroughs Wellcome Career Award at the Scientific Interface, Biomedical Engineering Society Rita Schaffer Young Investigator Award, Outstanding Young Scientist Award from the Maryland Academy of Sciences, Cellular and Molecular Bioengineering Young Innovator recognition, NSF CAREER Award, and the NIGMS Maximizing Investigators' Research Award.